

Leakage and Interpretability in Concept-Based Models

Enrico Parisini*

*The Alan Turing Institute
London, UK*

EPARISINI@TURING.AC.UK

Tapabrata Chakraborti

*The Alan Turing Institute
London, UK
University College London
London, UK*

TCHAKRABORTY@TURING.AC.UK

Chris Harbron

*Roche Pharmaceuticals
Welwyn Garden City, UK*

CHRIS.HARBON@ROCHE.COM

Ben D. MacArthur*

*The Alan Turing Institute
London, UK*

BMACARTHUR@TURING.AC.UK

Christopher R.S. Banerji*

*The Alan Turing Institute
London, UK
Kings College London
London, UK*

CBANERJI@TURING.AC.UK

*EP, BDM and CRSB should be considered joint corresponding authors. BDM and CRSB are joint senior authors.

Editor:

Abstract

Concept Bottleneck Models aim to improve interpretability by predicting high-level intermediate concepts, representing a promising approach for deployment in high-risk scenarios. However, they are known to suffer from information leakage, whereby models exploit unintended information encoded within the learned concepts. We introduce an information-theoretic framework to rigorously characterise and quantify leakage, and define two complementary measures: the concepts-task leakage (CTL) and interconcept leakage (ICL) scores. We show that these measures are strongly predictive of model behaviour under interventions and outperform existing alternatives in robustness and reliability. Using this framework, we identify the primary causes of leakage and provide strong evidence that Concept Embedding Models exhibit substantial leakage regardless of the hyperparameters choice. Finally, we propose practical guidelines for designing concept-based models to reduce leakage and ensure interpretability.

1 Introduction

Explainability and transparency are essential aspects of model design, especially in high-risk scenarios such as biomedical applications. Concept Bottleneck Models (CBMs) (Kumar et al., 2009; Lampert et al., 2009; Koh et al., 2020) stand out in the landscape of interpretable models as they learn a set of high-level intermediate concepts associated with an outcome, in a manner which facilitates human oversight (Banerji et al., 2025). CBMs first predict the level of activation of each concept for a given input data point, then use such activations to predict a task. Their structure makes them self-explainable, and allows for direct human supervision and intervention, as opposed to *post hoc* interpretability approaches.

In earlier CBMs, concept activations are real numbers (either probabilities or logits); more recently there have been efforts to generalise this approach to concept vector representations. Concept Embedding Models (CEMs, Espinosa Zarlenga et al., 2022) in particular are perceived as state-of-the-art in this regard.

A trained concept-based model, however, may be significantly less interpretable than expected, despite presenting the illusion of being so. A key reason for this is the phenomenon of *information leakage* (Kazhdan et al., 2021; Margeloiu et al., 2021; Mahinpei et al., 2021; Havasi et al., 2022). Leakage occurs when a poorly designed concept-based model uses additional information (such as interconcept relationships) to attain a higher task accuracy than a well-designed (i.e. transparent) concept-based model, at the cost of undermining concept interpretability. Storing such additional information into the learnt concepts is beneficial for the model with respect to loss function minimisation, as it typically allows the final head to leverage this information, attaining higher task performance while preserving high accuracy in concept predictions. This ultimately results in learnt concepts not being aligned with the ground-truth concepts, thus hindering the actual interpretability of the model. For example, in the clinical setting of cancer diagnosis, the grade of a tumour (how aggressive it looks under a microscope) is correlated to tumour stage (how much the cancer has spread through the body) and leakage may occur between learned concept representations of grade and stage. This means that a concept representation of grade might also contain information about tumour stage. However, these concepts have independent clinical definitions and their appropriate assessment is essential to guide clinical management. A concept-based model which displays leakage may therefore be unsafe for critical decision-making applications, such as clinical scenarios.

Contributions. We propose and test a framework based on information theory to assess the interpretability of concept-based models. In particular, we provide the first precise definition of information leakage, and identify two main ways it can manifest - as information leaking into each learnt concept from either the class label, or the other concepts. We accordingly define two measures, the concepts-task leakage (CTL) and the interconcept leakage (ICL) scores, and show that they

- are highly predictive of differences in performance upon intervention across models (the only robust indicator of interpretability in a CBM);
- substantially outperform previously proposed measures in terms of both predictiveness of leakage and robustness across models.

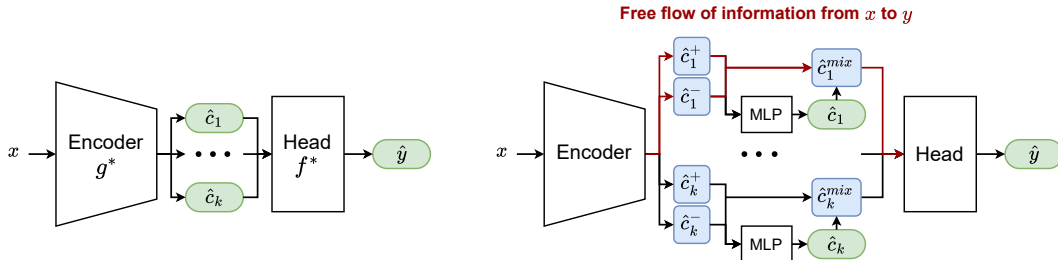


Figure 1: Scheme of CBM (*left*) and CEM (*right*) architectures. Quantities with green and blue backgrounds are predicted scalars and vectors respectively.

We then employ these measures to identify and assess the primary causes of leakage in CBMs, including over-expressive concept representations, an incomplete set of annotated concepts, a misspecified final head, and insufficient concept supervision. Building on this novel information-theoretic framework, we provide strong evidence that CEMs and closely related models exhibit dramatic leakage regardless of the choice of hyperparameters, thereby casting serious doubts on their interpretability. Finally, we propose a set of guidelines for the design of concept-based models based on preventing leakage, and we argue that evaluating leakage is a crucial step of model development to ensure interpretability.

Note: During the final stages of this work, Makonnen et al. (2025) appeared, presenting minor overlap with the content discussed here.

2 Concept bottleneck models

Consider a dataset $\{x^{(n)}, c^{(n)}, y^{(n)}\}_{n=1}^N$ with N observations, where $x^{(n)} \in \mathbb{R}^d$ is the input, $c^{(n)} \in \{0, 1\}^k$ represents a set of k annotated concepts, and $y^{(n)} \in \{1, \dots, \ell\}$ is the target label. A CBM (Figure 1) is the composition of a concept encoder g^* mapping the input to the predicted concept activations $\hat{c} = g^*(x)$, and a classifier head f^* which maps the concepts to the predicted label $\hat{y} = f^*(\hat{c})$. This framework easily extends to regression tasks y and to categorical or continuous concepts.

The presence of a concept bottleneck displaying the predicted concept activations for each input allows a human agent to directly supervise the model reasoning without resorting to post-hoc approaches to explainability such as CAM (Zhou et al., 2016), GradCAM (Selvaraju et al., 2017), LIME (Ribeiro et al., 2016) or SHAP (Lundberg and Lee, 2017). Additionally, this setup enables human interventions: if one or more predicted concepts are identified as incorrect for a given input $x^{(n)}$, a human agent can fix their values according to their expertise, resulting in an improved task prediction.

To achieve full interpretability, the final head architecture should represent a functional dependence that is interpretable. This allows for a higher level of supervision, e.g. in terms of which concepts are more relevant for the task prediction. A popular choice is linear classifiers.

There are three possible strategies to train CBMs as introduced by Koh et al. (2020):

- *independent training*, where the concept encoder and the final head are trained independently on ground-truth data,

$$g^* = \operatorname{argmin}_g \mathcal{L}_c(g(x), c), \quad f^* = \operatorname{argmin}_f \mathcal{L}_y(f(c), y), \quad (1)$$

where \mathcal{L}_c and \mathcal{L}_y are suitable loss functions for the concepts and the label respectively;

- *sequential training*, where the concept encoder is trained on ground-truth data, while the final head is trained on the predicted concepts,

$$g^* = \operatorname{argmin}_g \mathcal{L}_c(g(x), c), \quad f^* = \operatorname{argmin}_f \mathcal{L}_y(f(g^*(x)), y); \quad (2)$$

- *joint training*, where the model is trained end-to-end,

$$g^*, f^* = \operatorname{argmin}_{g,f} [\lambda \mathcal{L}_c(g(x), c) + \mathcal{L}_y(f(g(x)), y)], \quad (3)$$

with $\lambda \geq 0$ hyperparameter indicating the importance of concept learning over task learning. $\lambda = 0$ corresponds to a black box model.

Common choices for concept encoding include binary probabilities, soft probabilities or logits. We refer to *hard* CBMs as independently trained models with binary concept encoding, while *soft* CBMs denote jointly trained models with soft probability-based concept activations. Additionally, we refer to jointly trained models using logit-based concept encoding as *logit* CBMs.

More recently, CEMs (Figure 1) were proposed in Espinosa Zarlenga et al. (2022), where a pair of vectors $(\hat{c}_i^+, \hat{c}_i^-) \in \mathbb{R}^{2d}$ is predicted for each input and concept c_i , $i = 1 \dots k$ (with d hyperparameter indicating the embedding dimension). This pair of vectors is subsequently used to predict the activation \hat{c}_i as a soft probability. The weighted vectors $\hat{c}_i^w = \hat{c}_i \hat{c}_i^+ + (1 - \hat{c}_i) \hat{c}_i^-$ are then constructed and concatenated before being fed into the final head to predict the label. In this setup \hat{c}_i^+ and \hat{c}_i^- are meant to represent concept i being active or inactive respectively. Learning a two-fold representation for each concept enables interventions, by modifying the concept activations \hat{c}_i and thus selecting either \hat{c}_i^+ or \hat{c}_i^- as an input for the final head.

Training in CEMs is performed end-to-end; similar to joint CBMs, the loss function consists of reconstruction losses for both the concept activations and the class label, weighted by a parameter $\lambda \geq 0$ as in (3). To make such models more receptive to interventions (i.e. enhance the improvement in task performance after each intervention), they are exposed to interventions during training: each activation \hat{c}_i is set to its ground-truth value c_i with probability defined by a parameter $p_{int} \in (0, 1)$.

Reasoning in CEMs takes place at the level of the vectors \hat{c}_i^w , as opposed to CBMs where it is based on concept activations \hat{c}_i . However, as high-dimensional objects trained only to be predictive of concepts $c_i \in \{0, 1\}$, the vectors $\hat{c}_i^w \in \mathbb{R}^d$ are excessively flexible representations, capable of encoding an arbitrary amount of information about the task label. We demonstrate in Section 8 that this is the fundamental reason why CEMs generally fail to be interpretable for any choice of their hyperparameters. While Espinosa Zarlenga et al. (2022) presents CEMs as interpretable models that resolve the accuracy-interpretability trade-off,

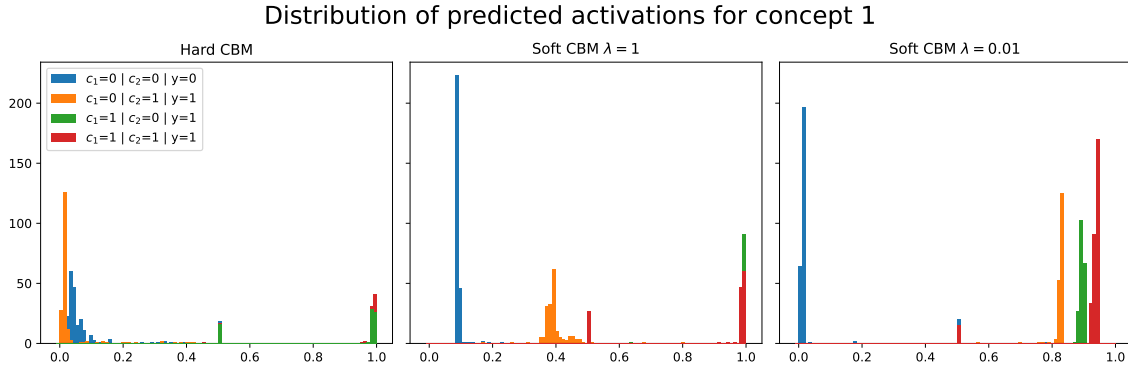


Figure 2: Distributions of predicted activations for concept 1 on the test set in CBMs with increasing leakage from left to right. Colours are based on the ground-truth values of concepts and task label.

they still adhere to this trade-off in favour of accuracy, effectively sacrificing interpretability. Although requiring a case-by-case evaluation, other CEM-based architectures, such as Espinosa Zarlenga et al. (2023b); Ridzuan et al. (2024); Gao et al. (2024); Hu et al. (2024); Srivastava et al. (2024), are likely to face similar interpretability challenges.

3 Definition of leakage

The explainability of CBMs and CEMs assumes that learnt concepts are aligned with ground-truth human-interpretable concepts. However, on general grounds that is not the case. During training, concept-based models often encode additional input information into the learned concepts to enhance task accuracy - *information leakage* occurs (Kazhdan et al., 2021; Margeloiu et al., 2021; Mahinpei et al., 2021; Havasi et al., 2022; Lockhart et al., 2022; Ragkousis and Parbhoo, 2024). The model is not relying solely on the value of concepts for its task prediction, but also on such leaked information, hindering interpretability. The reasoning of the model thus becomes effectively obscure to human agents, to a degree specified by the amount of leakage.

In practice leakage manifests as additional structure arising in the learnt concept distributions, as showcased in Figure 2. In this example models must learn two binary concepts for a binary classification task (see Appendix A.1 for more details). We compare the distributions of activations for the first concept by a hard CBM and two soft CBMs, with either intermediate ($\lambda = 1$) or low ($\lambda = 0.01$) concept supervision. By definition no leakage can be present in hard CBMs, since concept learning is independent of task learning, and concepts are converted to binary values before being passed to the final head, preventing leaked information. Soft CBMs with lower concept supervision are instead more prone to leakage as accurate concept learning is not enforced during training (see Koh et al., 2020; Kazhdan et al., 2021, and our results in Section 7).

Neglecting the peak close to 0.5 corresponding to observations the model is most uncertain about, the concept distribution in the hard CBM is very close to the binary ground-truth distribution for concept 1. In the soft CBM with $\lambda = 1$ additional structure is learnt

based on the value of the other concept and of the class label, while for $\lambda = 0.01$ the concept itself is a very strong predictor of the value of both the class label and the other concept. In particular, the distribution is more similar to the ground-truth binary task distribution than to the concept distribution.

We identify two main types of leakage that concept-based models resort to:

1) *Concepts-task leakage*: additional information about the task is stored into the learnt concepts. For training to be successful, the annotated concepts must be predictive of the task label as measured by the ground-truth mutual information (MI) between each concept and the task label. If concepts-task leakage is present, learned concepts-task MI is higher than ground-truth concepts-task MI. This is usually the prominent type of leakage and the main cause of non-interpretability, as it directly allows the model to achieve a better task performance (see experiments in Section 6).

2) *Interconcept leakage*: additional information about the other concepts is stored into each concept. In a given dataset, concepts are predictive of the value of other concepts as determined by their ground-truth pair-wise MI. This type of leakage manifests as learned concepts being more predictive of the value of the other learned concepts, resulting in a learned interconcept MI being higher than the ground-truth. This effect is usually a secondary factor of non-interpretability (see experiments in Section 6), but it may be beneficial for models as an internal error-correcting tool: interconcept leakage provides redundant pathways for the model to attain high task performance even when concept predictions are poor.

This classification, highlighting the information-theoretic nature of leakage, forms the foundation of our quantitative approach to detect and measure it.

4 Existing measures of interpretability and their shortcomings

Previous works (Koh et al., 2020; Kazhdan et al., 2021; Margeloiu et al., 2021; Mahinpei et al., 2021; Havasi et al., 2022; Espinosa Zarlenga et al., 2023a) have proposed several measures of leakage, however none take into account the information-theoretic nature of leakage outlined in Section 3. As we highlight in this section, these existing measures consequently exhibit inherent limitations in sensitivity and robustness, resulting in a lack of applicability to real-world scenarios.

Concept performance metrics. Although performance metrics such as concept accuracy, F1 score and AUC are general quality indicators of concept learning, they are not sensitive to more subtle effects undermining interpretability such as leakage. In particular, two models may exhibit the same evaluation scores while considerably differing in terms of leakage. This is apparent from the example in Figure 2, where a classification threshold of 0.5 yields essentially the same concept accuracy and F1 score for the hard and $\lambda = 1$ soft CBM, while the latter encodes a non-trivial amount of additional structure. Concept AUC is a finer measure of interpretability than accuracy and F1 score as it captures more information about the concept distribution, and in this simple example it is able to discriminate between those two models. However it is not generally sensitive enough to quantify leakage in more complex setups as we illustrate in Section 6.

OIS and NIS. These scores were defined in Espinosa Zarlenga et al. (2023a). The Oracle Impurity Score (OIS) is obtained by training $k(k - 1)$ additional neural networks (NNs) $\psi_{i,j}$ (typically 2-layer perceptrons of modest size) predicting the value of the ground-truth concept j from the learnt representation of concept i . The $k \times k$ impurity matrix defined as $\pi_{ij}(\hat{c}, c) = AUC(\psi_{i,j}(\hat{c}_i), c_j)$ is meant to estimate the predictivity of each learnt concept representation with respect to any other across the dataset. The OIS is the average difference between the predictivities of learnt and ground-truth concepts over pairs of concepts,

$$\text{OIS}(\hat{c}, c) = \frac{2}{k} \|\pi(\hat{c}, c) - \pi(c, c)\|_F, \quad (4)$$

where $\|\cdot\|_F$ indicates the Frobenius norm, and the normalisation ensures $0 \leq \text{OIS} \leq 1$. The OIS is thus intended to provide an estimate of interconcept leakage, while being unable to account for concepts-task leakage, which is the prevalent effect as we illustrate in Section 6. Although demonstrated to be superior to other concept-quality metrics in Espinosa Zarlenga et al. (2023a), the OIS is subject to additional limitations that hinder its applicability. In particular, in Section 6 we prove that

1. its value is typically non-vanishing and relatively high for hard CBMs, indicating biases and a lack of sensitivity;
2. due to the intrinsic stochasticity in its definition which involves training NNs, it is extremely variable when repeatedly evaluated for a given model at test time. The resulting broad confidence intervals typically prevent drawing any statistically significant conclusion when comparing models with different amounts of leakage, ultimately limiting the utility of this score for model design.

The Niche Impurity Score (NIS) was defined to capture leakage manifesting as additional information about concept j stored into a joint subset of the learnt representations $\{i_1, \dots, i_p\}$ not containing concept j (see Espinosa Zarlenga et al., 2023a, for details). Such a score is meant to go beyond pair-wise interconcept leakage and estimate the (generally subdominant) higher-order effects. As illustrated in Appendix B, the NIS is generally non-vanishing and very high for hard CBMs, and moreover it appears to be anticorrelated with intervention performance and leakage. As such, we deem it unsuitable to measure leakage and interpretability.

Performance upon intervention. Intervention performance can be measured at test time by substituting the ground-truth concept values to the predicted activations, with a given policy defining the order of the concepts to intervene on. The behaviour of the task accuracy after each intervention measures to what extent learnt and ground-truth concepts are aligned. A task accuracy that decreases is a coarse indication of leakage: the final head

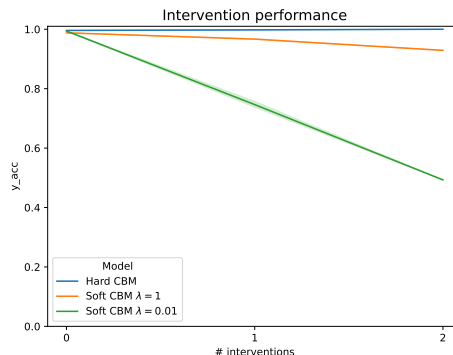


Figure 3: Performance upon random intervention of the three models analysed in Figure 2.

expects additional information that is not present in the ground-truth concept distribution. Figure 3 shows the intervention performance of the same three models as in Figure 2. Models with higher leakage have worse performance, while the hard CBM displays a monotonically increasing task accuracy.

As a metric of leakage, intervention performance has however several limitations.

1. Being based on evaluation scores, it does not address the information-theoretical nature of leakage, resulting in a limited resolution. It is unable to distinguish between interconcept and concepts-task leakage, and it does not directly quantify interpretability at the level of single concepts. Typically it is thus not sufficiently informative to guide model design and hyperparameter selection.
2. Its evaluation is computationally expensive, especially in real-world applications where models have a large number of concepts and are evaluated using state-of-the-art policies with a high overhead such as CooP (Chauhan et al., 2023).
3. In more complex architectures such as CEMs, it is not a measure of interpretability, see Appendix H.

Poor intervention performance is in particular a measure of leakage with perfect specificity (leakage has always occurred when performance is poor), but with poor sensitivity (when performance is good, leakage is not guaranteed to be absent). Although the leakage scores we propose in Section 5 address these issues, intervention performance generally remains a coarse but useful indicator of leakage in CBMs. Let us denote by $y_{acc}^{*(k)}$ the task accuracy after all the k concepts have been intervened on in the model under evaluation, which coincides with the accuracy of the final head on the ground-truth concepts. As a benchmark of the proposed leakage scores we will use the intervention score

$$S_{(int)} = y_{acc}^{(k)} - y_{acc}^{*(k)}, \quad (5)$$

where $y_{acc}^{(k)}$ is the reference accuracy of the final head when separately trained on the ground-truth concepts. It represents the maximal task accuracy attainable by the final head and it measures the fundamental misspecification of the final head with respect to the ground-truth functional dependence $y = f(c)$. $S_{(int)}$ thus quantifies the further decrease in task accuracy caused by leakage on top of the possible final head misspecification. Its value is independent of the intervention policy adopted. Note that $y_{acc}^{(k)}$ coincides with $y_{acc}^{*(k)}$ for a successfully trained hard model, thus $S_{(int)} = 0$ for hard models by construction.

5 Concepts-task and interconcept leakage scores

Leakage is information-theoretic in nature and as such, it can be captured appropriately only by metrics based on quantities from information theory. As discussed in Section 3, the leaked information and the corresponding additional structure in the learnt concept distributions can be measured as modifications in the ground-truth interconcept and concepts-task MIs respectively. This motivates the definition of the following set of scores based on information theory to quantify leakage and the interpretability of concept-based models, and overcome the limitations of the existing measures.

Concepts-task leakage scores. Denoting by $H(z)$ the entropy of the variable z and by $I(z, w)$ the MI between the variables z and w , we define the concepts-task leakage score for concept i as the difference between predicted and ground-truth MIs between concept i and the task label,

$$CTL_i(\hat{c}, c, y) = \left| \frac{I(\hat{c}_i, y)}{H(y)} - \frac{I(c_i, y)}{H(y)} \right|. \quad (6)$$

This score quantifies the additional information that the learnt concept i encodes about the task label with respect to ground-truth. MIs are appropriately normalised by the entropy of the class label to ensure $0 \leq CTL_i \leq 1$. We further define the average concepts-task leakage score

$$CTL(\hat{c}, c, y) = \frac{1}{k} \sum_{i=1 \dots k} CTL_i(\hat{c}, c, y), \quad (7)$$

as the average extra information about the task stored into the learnt concepts.

Interconcept leakage scores. In a similar fashion, we define the pairwise interconcept leakage score between concepts i and j as

$$ICL_{ij}(\hat{c}, c) = \left| \frac{I(\hat{c}_i, \hat{c}_j)}{\sqrt{H(\hat{c}_i) H(\hat{c}_j)}} - \frac{I(c_i, c_j)}{\sqrt{H(c_i) H(c_j)}} \right|, \quad (8)$$

which measures the additional predictivity of the learnt concept i for concept j with respect to ground-truth. The normalisation by the entropies also in this case ensures $0 \leq ICL_{ij} \leq 1$, and note that $ICL_{ii} = 0$ since $I(z, z) = H(z)$. We also define the per-concept and average interconcept leakage scores

$$ICL_i(\hat{c}, c) = \frac{1}{k-1} \sum_{j=1 \dots k} ICL_{ij}(\hat{c}, c), \quad ICL(\hat{c}, c) = \frac{1}{k} \sum_{i=1 \dots k} ICL_i(\hat{c}, c), \quad (9)$$

to quantify the extra information that each concept encodes about the other concepts, and the average additional interconcept predictivity respectively.

The CTL and ICL scores are meant to summarise complementary aspects of the leakage present in a given concept-based model, as well as its overall interpretability. We define the following criterion to detect leakage using the proposed scores:

Leakage Criterion. *When comparing two models (or two model classes) A and B , a sufficient condition for A having higher leakage than B is that either of the following conditions are satisfied,*

- *both the CTL and ICL scores are higher in A than in B with high statistical confidence,*
- *either the CTL or the ICL score is higher in A with high statistical confidence, while the other score takes compatible values in A and B .*

Note that this is a conservative criterion covering the majority of cases, while it cannot be used in the cases where one measure is higher in A and the other is lower in B (or vice versa) with high statistical confidence.

The CTL_i , ICL_{ij} and ICL_i measures convey more detailed information about each type of leakage at the level of single concepts. This is particularly useful for model design and when performing interventions (as they essentially indicate the risk of intervening on each concept). The framework above can be applied to concept-based models with a range of concept encodings, including binaries, soft probabilities, logits and vector representations. Alternative normalisations of MI can be used, although we found those adopted in (6) and (8) to be particularly transparent from an information theory perspective, and robust in the experiments carried out. We estimate MI and entropy using the KSG estimator (Kraskov et al., 2004), based on k -nearest neighbour statistics.

6 Robustness of leakage scores

We now demonstrate the robustness of the CTL and ICL scores and how they overcome the issues of the existing measures of leakage.

Datasets. For our experiments we consider three synthetic datasets, TabularToy(δ), dSprites(γ) and 3dshapes(γ), presented in Espinosa Zarlenga et al. (2023a). TabularToy(δ) is a binary-class tabular dataset based on the dataset from Mahinpei et al. (2021), while dSprites(γ) and 3dshapes(γ) are multi-class image-based datasets building upon dSprites (Matthey et al., 2017) and 3dshapes (Burgess and Kim, 2018) respectively. The use of synthetic datasets enables us to (i) modify the functional dependence $y = f(c)$ and hence tune the ground-truth concepts-task MI, and furthermore (ii) tune the ground-truth interconcept MI via the parameters $\delta \in (0, 1)$ and $\gamma \in \{0, \dots, 4\}$ in dSprites and $\in \{0, \dots, 5\}$ in 3dshapes). See Appendix A for more details on the experimental setup.

CTL and ICL are highly sensitive to leakage. We consider pairs of models encoding different levels of leakage as assessed by intervention performance (Figure 4). The models in each pair were chosen to have essentially identical concepts and task evaluation scores (Table 1), evidencing the severe limitations of these metrics in capturing leakage. In all cases the CTL and ICL scores correctly detect the different amounts of leakage according to the Leakage Criterion, with no level of uncertainty. On the contrary, we note as a general behaviour that the large confidence intervals of the OIS prevent drawing any statistically significant conclusion on leakage. Appendix C presents the concept-wise leakage scores for these models and illustrates how they provide more fine-grained information at the level of individual concepts.

CTL and ICL are vanishing for hard CBMs. Figure 5 shows the leakage scores for hard models trained on a number of datasets in both low and high regimes of ground-truth interconcept MI. By construction hard CBMs have vanishing leakage (Koh et al., 2020; Kazhdan et al., 2021; Margeloiu et al., 2021), and the CTL and ICL scores are in all cases compatible with zero, regardless of the interconcept MI. The OIS is instead non-vanishing in all experiments, failing to meet a fundamental requirement of leakage metrics. We further note that for each dataset its estimated values on hard CBMs are comparable to those on the models shown in Figure 4, which instead encode a significant amount of leakage. This represents further evidence of the limitations of the OIS in distinguishing interpretable from uninterpretable concept-based models.

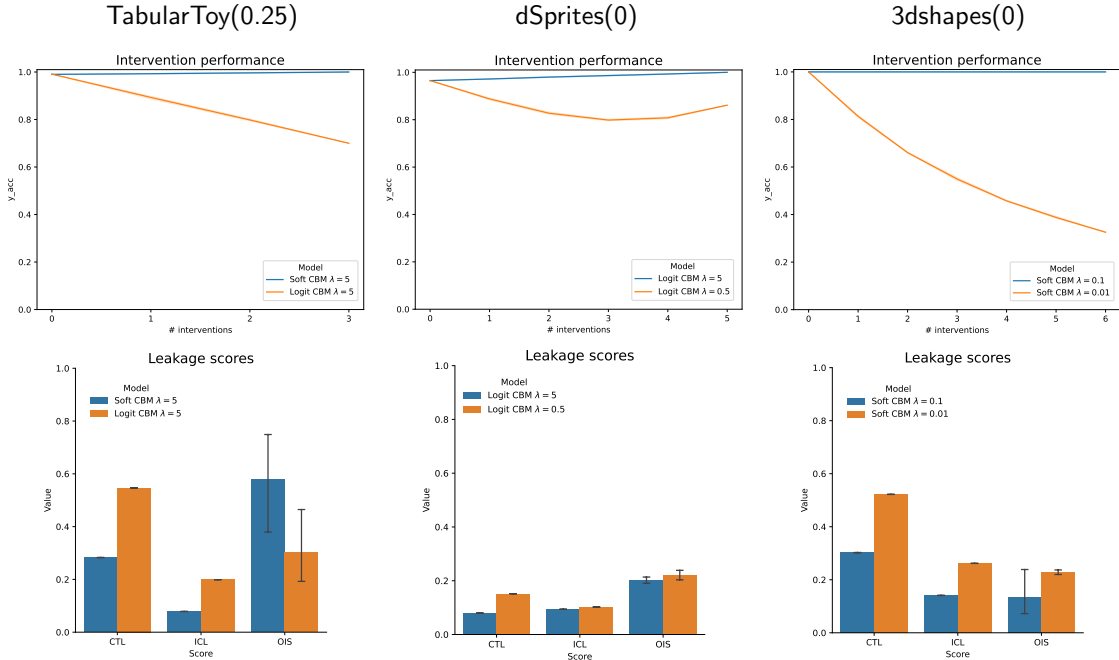


Figure 4: Intervention performance and leakage scores computed for pairs of soft and logit CBMs with different amounts of leakage but similar evaluation scores (see Table 1) trained on TabularToy(0.25), dSprites(0) and 3dshapes(0). Metrics are evaluated on a 5-fold basis for each model.

		c_{acc}	c_{F1}	c_{AUC}	y_{acc}	y_{F1}	y_{AUC}	$S_{(int)}(\downarrow)$
TabularToy(0.25)	Soft CBM $\lambda = 5$	0.993	0.992	0.992	0.990	0.990	0.990	0.000
	Logit CBM $\lambda = 5$	0.995	0.995	0.995	0.991	0.991	0.991	0.301
dSprites(0)	Logit CBM $\lambda = 5$	0.993	0.993	0.993	0.965	0.976	0.698	0.000
	Logit CBM $\lambda = 0.5$	0.992	0.992	0.992	0.965	0.975	0.689	0.139
3dshapes(0)	Soft CBM $\lambda = 0.1$	1.000	1.000	1.000	1.000	1.000	0.201	0.000
	Soft CBM $\lambda = 0.01$	1.000	1.000	1.000	1.000	1.000	0.207	0.674

Table 1: Concept and task evaluation scores, as well as intervention scores of pairs of soft and logit CBMs with different levels of leakage (see Figure 4).

CTL and ICL strongly correlate with intervention performance. We train a number of soft and logit CBMs on each dataset in both high and low regimes of ground-truth interconcept MI and with different levels of concept supervision (see Appendix D for details on this experiment). The evaluation of the OIS, ICL and CTL scores is repeated 5 times for each individual model yielding an uncertainty on their value. We then Monte-Carlo (MC) sample 10K times from the uncertainty distributions of each score (assuming normality), and for each sample we compute the Pearson r coefficient between each score and the intervention score $S_{(int)}$. The resulting distribution of Pearson r values between

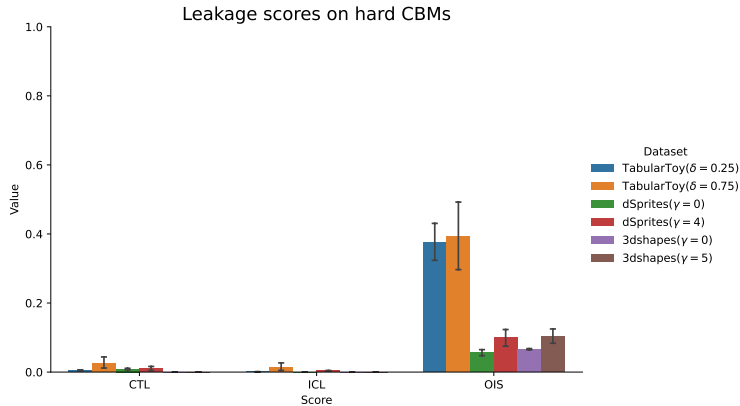


Figure 5: Leakage scores evaluated on hard CBMs on datasets with high and low ground-truth interconcept MI. The 95% confidence intervals are obtained from a 5-fold training on each dataset.

	CTL		ICL		OIS	
	Pearson r	$-\log_{10}(p)$	Pearson r	$-\log_{10}(p)$	Pearson r	$-\log_{10}(p)$
TT(0.25)	0.75 ± 0.05	2.6 ± 0.4	0.69 ± 0.07	2.1 ± 0.5	0.49 ± 0.11	1.1 ± 0.4
dS(0)	0.83 ± 0.06	3.6 ± 0.8	0.68 ± 0.07	2.0 ± 0.5	0.69 ± 0.07	2.2 ± 0.5
3ds(0)	0.84 ± 0.02	4.0 ± 0.3	0.86 ± 0.03	4.4 ± 0.5	0.81 ± 0.04	3.9 ± 0.7
TT(0.75)	0.55 ± 0.05	1.3 ± 0.2	0.55 ± 0.12	1.4 ± 0.5	0.27 ± 0.13	0.5 ± 0.3
dS(4)	0.70 ± 0.09	2.2 ± 0.6	0.45 ± 0.08	1.0 ± 0.3	0.55 ± 0.10	1.3 ± 0.5
3ds(5)	0.75 ± 0.04	2.9 ± 0.4	0.24 ± 0.15	0.5 ± 0.5	0.70 ± 0.07	2.5 ± 0.6

Table 2: Pearson r coefficients and corresponding p -values measuring the correlations of CTL, ICL and OIS metrics against $S_{(int)}$. To better capture the scores distributions resulting from MC sampling, the displayed uncertainties are standard deviations. Significant and highly significant correlations correspond to $-\log_{10}(p) \simeq 1.3$ and 2.0 respectively.

each leakage score and intervention performance across models and for each dataset provides an estimate of its uncertainty, while the corresponding distribution of p -values provide information about the significance of correlation.

Table 2 reports the mean and standard deviation of the resulting Pearson r and p -value distributions. The proposed CTL and ICL scores highly correlate with intervention performance and they systematically outperform OIS across datasets and robustly to ground-truth interconcept MI. This analysis also quantifies the importance of concepts-task and interconcept leakage in each case. CTL generally appears as the prominent form of leakage over ICL. Its correlation with intervention performance is typically stronger than ICL, and is moreover significant in all datasets and highly significant in 5 out of 6 datasets. This behaviour reflects the optimization pressure favouring the storage of additional task-relevant information in the learnt concepts rather than information about the other concepts, to achieve a better task performance. Nevertheless, these results are evidence that also interconcept leakage systematically arises during model training, in particular displaying correlations of comparable magnitude to concept-task leakage in 3 out of 6 datasets.

7 Causes of leakage

The proposed information-theoretic leakage scores are robust and sensitive and can thus be used to identify the most common causes of leakage and assess their impact on interpretability.

A first effect that directly impacts the interpretability of a concept-based model is the concept encoder being misspecified with respect to the target concept distribution. When such a misspecification is significant, the model is essentially not capable of learning concepts and their relations. This may favour the emergence of additional issues, such as non-locality (Raman et al., 2023; Huang et al., 2024). Concept-based architectures enforcing accurate learning of interconcept relations have been recently proposed (Kim et al., 2023; Vandenhirtz et al., 2024; Xu et al., 2024; Kim et al., 2025). We recognise however that this problem is significantly use-case specific and it is usually sufficient to opt for a concept encoder with an improved architecture to solve it. In the following experiments we will thus consider concept encoders that are sufficiently well-specified.

Insufficient concept supervision. When λ is set to be small, during training the model is encouraged to achieve better task performance at the cost of poor concept learning and high leakage. This issue was originally observed in Koh et al. (2020), where poor intervention performance was found when training models with low λ . To precisely quantify this effect, we train soft and logit CBMs with low, intermediate and high values of λ on datasets with both low and high interconcept MI. The resulting leakage scores displayed in Figure 6 confirm that leakage decreases as we enhance concept supervision.

However, as detailed in Appendix E, leakage does not fall to zero as one keeps increasing λ – the leakage scores reach a non-vanishing minimal value, specific to each model class. At higher values $\lambda \gtrsim 10$, models focus excessively on concept learning, and the task objective may be poorly learnt. This results in a drop in task performance or an increase in leakage. Each model class has thus an associated optimal range of $\lambda \in (\lambda_{min}, \lambda_{max})$ where the minimal amount of leakage is attained, below which models exhibit proportionally higher leakage and above which training often fails. As evidenced by our results, such an optimal interval can be identified using the CTL and ICL scores.

Over-expressive concept encoding. When the chosen concept representation is significantly more expressive than the annotated concept representation, during training the model is generally encouraged to misuse the surplus expressivity to store additional information into concepts to ease task predictions. This is evidenced in Figure 6 where annotated concepts are binary, while learnt concepts are soft probabilities and logits, and as such over-expressive for the setup. We note that raising λ is less effective at decreasing leakage when concepts representations are more expressive, as in the logit models, and furthermore the minimal attainable leakage is significantly higher for such models over soft CBMs. This behaviour casts doubts on the advantages of vector concept encodings when ground-truth concepts are binary, and we will see in Section 8 how these concerns impact and are substantiated in CEMs. Finally, we observe that models with low λ generally have a comparable level of high leakage regardless of the concept encoding.

Incomplete set of concepts. When the set of annotated concepts is incomplete for the task, meaning that it is not sufficiently predictive, models tend to encode the information

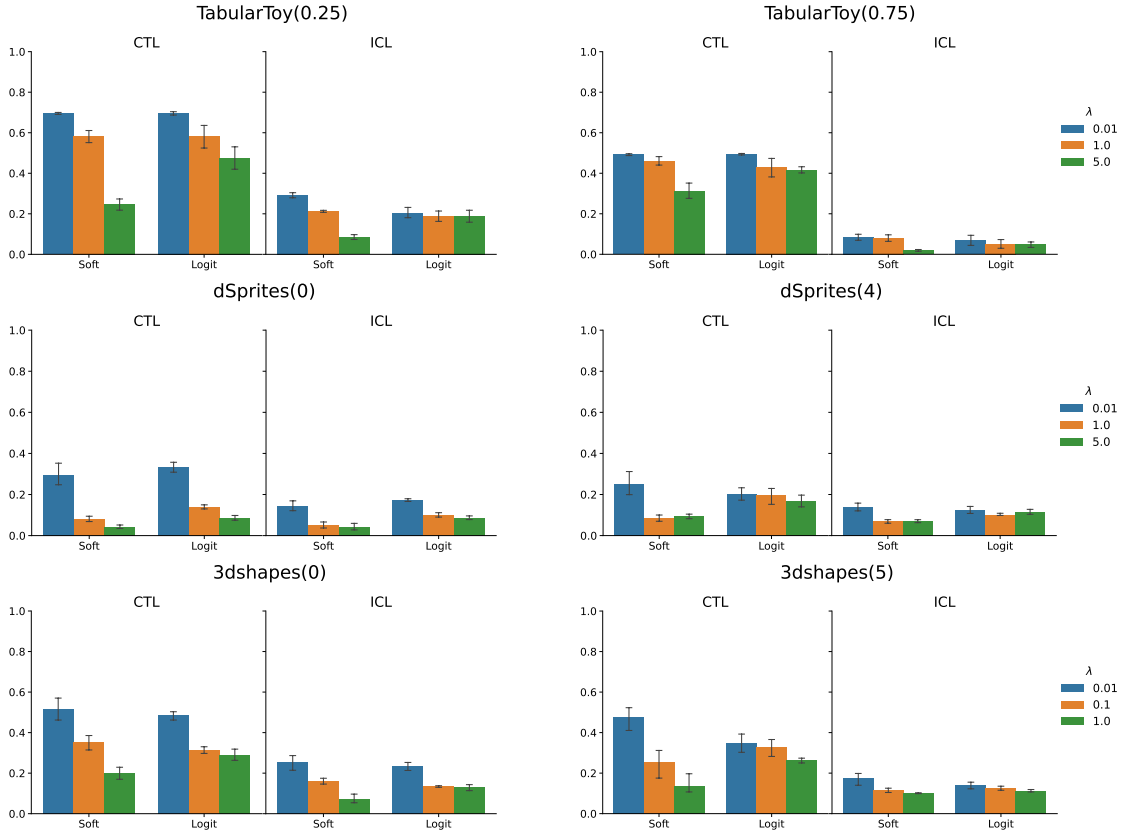


Figure 6: Leakage scores evaluated for soft and logit models with different levels of concept supervision, on datasets with low (*left*) and high (*right*) ground-truth interconcept MI.

about the missing concepts (or generally additional information that may be required) into the learnt concepts to nonetheless achieve a high task performance. This translates into sizeable leakage and a loss of interpretability. This issue has been discussed in previous works (Kazhdan et al., 2021; Margeloiu et al., 2021; Mahinpei et al., 2021; Havasi et al., 2022).

To accurately assess this phenomenon using our information-theoretic scores, we train soft CBMs with low, intermediate and high levels of concept supervision on a range of datasets with roughly one third of concepts removed (see Appendix A for more details on which concepts are removed for each dataset). This results in a sizeable decrease of the reference task accuracy $y_{acc}^{(k)}$ of the final head trained on the ground-truth concepts introduced in equation (5) (Table 3, left). The leakage scores of the trained models are displayed in Figure 7, along with those of models with complete sets of concepts for comparison. Their concepts and task accuracies are presented in Appendix F.

According to the Leakage Criterion, we detect more leakage in 9/9 model classes trained on incomplete sets of concepts. At low and intermediate λ , there is considerably more leakage in models trained on an incomplete set. At high lambda, CTL scores are typically

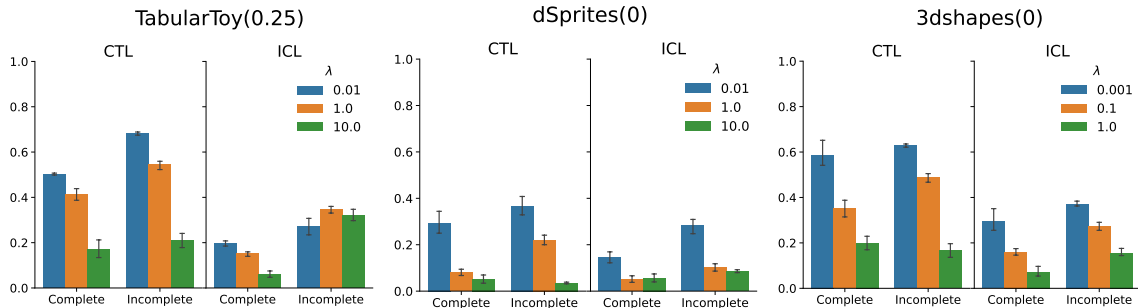


Figure 7: Leakage scores evaluated for soft CBMs at different levels of concept supervision, on datasets with complete and incomplete sets of concepts.

$y_{acc}^{(k)}$	complete	incomplete	well-specified	misspecified
TabularToy(0.25)	1.000 ± 0.000	0.786 ± 0.000	1.000 ± 0.000	0.687 ± 0.000
dSprites(0)	1.000 ± 0.000	0.749 ± 0.004	1.000 ± 0.000	0.807 ± 0.000
3dshapes(0)	1.000 ± 0.000	0.655 ± 0.002	1.000 ± 0.000	0.859 ± 0.008

Table 3: Former two columns: baseline $y_{acc}^{(k)}$ task accuracies of final heads trained on datasets with complete and incomplete sets of concepts. Latter two columns: baseline $y_{acc}^{(k)}$ task accuracies of a linear head on the linear (*well-specified*) and non-linear (*misspecified*) ground-truth task labels. We report 95% confidence intervals over 5-fold training.

comparable in models with incomplete and complete concept sets, while ICL remains significantly higher in case of an incomplete concept set.

Misspecified final head. If the final head is not flexible enough to learn sufficiently well the ground-truth $y = f(c)$ dependence, during training the model tends to store the necessary dependences into the learnt concepts, which get deformed to encode additional information about the task and the other concepts. In real-world applications a common choice for the final head of a CBM is a linear layer, which being itself interpretable, allows in principle for a full model explainability. In reality the task is however very often described by a highly non-linear function of the concepts, and a linear layer can be severely misspecified in such cases.

As an example showcasing the general effects of final head misspecification as well as representing a potential shortcoming of a considerable fraction of existing CBMs, we consider soft CBMs with a linear head trained on datasets where the ground-truth task is either a linear or non-linear function of the concepts. To achieve that, we modify the functional dependences in TabularToy(0.25), dSprites(0) and 3dshapes(0) by adding non-linear terms to the original tasks – see Appendix A.1. As a baseline measuring the final head misspecification, for each dataset we train a separate linear head on the ground-truth concepts. Table 3 shows the resulting decrease in task performance in terms of the reference task accuracy $y_{acc}^{(k)}$. The corresponding leakage scores are displayed in Figure 8 and their concepts and task accuracies are presented in Appendix F. According to the Leakage Criterion, a misspecified final head causes a higher leakage in 7/9 model classes. Note in particular that high concept

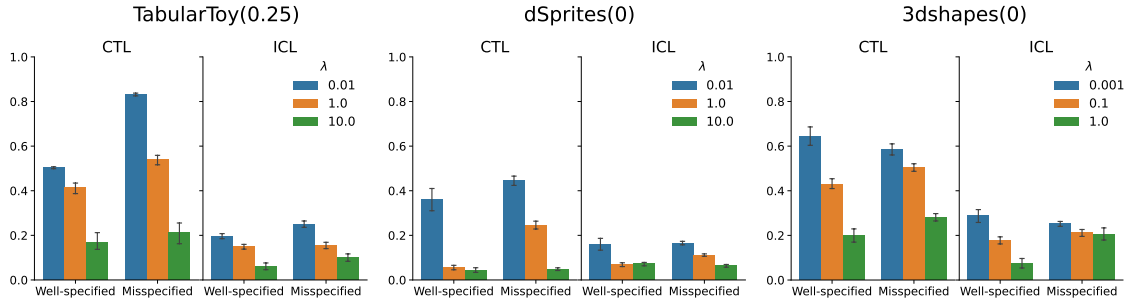


Figure 8: Leakage scores evaluated for soft CBMs with a linear final head trained on datasets where the task is either a linear (*Well-specified*) or a non-linear (*Misspecified*) function of the concepts, at low, intermediate and high levels of concept supervision.

supervision is generally not sufficient to compensate for the additional leakage induced by the final head misspecification.

8 CEMs are not interpretable

CEMs (Espinosa Zarlenga et al., 2022) have gained significant recognition in the domain of interpretable concept-based modelling. However, due to their inherent design these models present fundamental interpretability issues. The primary cause of this is the fact that their reasoning is based on data point-dependent concept vector representations, and not directly on concept activations as in CBMs.

Consider a dataset where the annotated concepts are binary.¹ A transparent concept-based model trained on such a dataset must generate task predictions solely based on the activation levels of concepts (essentially whether each of them is on or off), which can be supervised during training and later by a human agent. The vector representations \hat{c}_i^w on which CEMs reasoning is based are instead high-dimensional objects capable of encoding an enormous amount of information besides concept activations. Therefore, the necessary condition for CEMs to be deemed interpretable is that the learnt embeddings must be faithful representations of concepts, corresponding to the situation where the generated vectors \hat{c}_i^w essentially contain the same information as the annotated concepts (were these binary, categorical or continuous).²

However, in this section we demonstrate that the learnt embeddings in CEMs are *not* a faithful representation of concepts and that they encode large amounts of leaked information. Intuitively, this is a consequence of no *direct* supervision being performed on the actual input of the final head, but only on the predicted concept activations \hat{c}_i via the

1. The following argument straightforwardly extends to categorical and continuous annotated concepts.
2. Note that there would be limited advantages in using vector representations if that were the case and they were hence just as informative as concept activations. Besides introducing extra computational overhead during training and inference, the fact that the final head takes as input the concatenated vectors \hat{c}_i^w limits interpretability of the $y = f(c)$ functional dependence, even when interpretable final heads such as a linear layer are used. The final head reasons at the level of the each vector component, which are not interpretable, and statements that can be made are of the form, *the m -th component of the i -th concept vector is more relevant for the task prediction than the n -th component of the j -th concept vector.*

concept reconstruction loss. This means that in the forward pass, an arbitrary amount of information is allowed to flow undisturbed from the input x to the task prediction through the concept vectors, as long as the embeddings \hat{c}_i^+ and \hat{c}_i^- generated from x are predictive of the single scalar c_i . Information is free to leak into the learnt vectors, fundamentally obscuring the model reasoning and effectively resulting in a scenario where the model is a black box whose explainability can be only partially recovered using *post-hoc* methods. This fundamental problem of CEMs is further exacerbated by our findings from Section 7 concerning over-expressive concept representations with respect to the annotated concepts, and in particular how such setups generally favour leakage.

Using our information-theoretic approach, we now show in detail how the learnt concept embeddings are affected by concepts-task leakage for any choice of the hyperparameters. Moreover, we find that contrarily to what happens in CBMs, higher concept supervision actually results in *higher* interconcept leakage.

Information-theoretic measures to assess CEMs interpretability. CEMs incorporate several concept representations – the concept probabilities \hat{c}_i just as CBMs, as well as the vector encodings \hat{c}_i^+ , \hat{c}_i^- and \hat{c}_i^w . Reasoning happens at the level of the weighted vectors \hat{c}_i^w , making them critical objects where leakage could hinder interpretability. As described in Appendix G, entropy and MI estimators are generally affected by biases depending on the dimension of variables. This entails that one cannot compare quantities estimated for concept representations of different dimensions, as required by the definitions of the CTL and ICL scores in equations (6)-(8), which in this case would involve subtracting normalised MIs estimated on the ground-truth concepts c_i from those on the vectors \hat{c}_i^w . To assess leakage in CEMs, it will be sufficient to analyse the behaviour of the normalised MIs on \hat{c}_i^w across different models without referring to ground-truth normalised MIs, and such a bias will not affect our discussion.

We define the concepts-task normalised MI between each vector \hat{c}_i^w and the task label, averaged across the k concepts,

$$\tilde{I}^{(CT)}(\hat{c}^w, y) = \frac{1}{k} \sum_{i=1}^k \frac{I(\hat{c}_i^w, y)}{H(y)}. \quad (10)$$

This score captures how informative on average the weighted vectors \hat{c}_i^w are of the task, and it represents a simpler version of the CTL score without the ground-truth concepts-task MI as a reference.

In a similar spirit to the ICL scores, one can further define a metric capturing the amount of information that a concept representation \hat{c}_i^w encodes about the other concepts. Averaged over the $k(k-1)/2$ non-trivial concept pairs, such interconcept normalised MI takes the form,

$$\tilde{I}^{(IC)}(\hat{c}^w, c) = \frac{2}{k(k-1)} \sum_{i=1}^k \sum_{j<i} \frac{I(\hat{c}_i^w, c_j)}{H(c_j)}. \quad (11)$$

Note that differently from the ICL scores, $\tilde{I}^{(IC)}$ does not measure how much a learnt concept representation is predictive of another one. This approach, based on annotated concepts instead, has the benefit of limiting the overall dimensionality of the space used to estimate

MIIs (in this case $d + 1$ instead of $2d$), mitigating the effects of the dimensional-dependent bias.

An auxiliary quantity that in the case of higher-dimensional representations contains non-trivial information is the normalised MI of a concept representation $\hat{\mathbf{c}}_i^w$ with the value of the corresponding ground-truth concept c_i . Its average over the k concepts reads,

$$\tilde{I}^{(\text{self})}(\hat{\mathbf{c}}^w, c) = \frac{1}{k} \sum_{i=1}^k \frac{I(\hat{\mathbf{c}}_i^w, c_i)}{H(c_i)}, \quad (12)$$

providing a measure of how predictive each concept representation is of its own concept.

Concepts-task leakage affects every CEM. If the vectors $\hat{\mathbf{c}}_i^w$ learnt by CEMs were a faithful representation of concepts, they should be clustered based on the value of the annotated concepts c_i only. To test this idea, we train CEMs with a range of λ and p_{int} , on TabularToy(0.25), dSprites(0) and 3dshapes(0). As we show in Figure 9 (see Figure 25 for similar results at non-vanishing p_{int}), this is never the case: although concepts are binary in these experiments, instead of two homogeneous clusters for each concept, we find a rich structure based on the ground-truth value of the task label, for any λ and p_{int} . This parallels the additional structure appearing in the concept distributions of CBMs affected by leakage, here in the case of a higher dimensional concept representation. This behaviour can be tracked back to the fact that the vectors $\hat{\mathbf{c}}_i^w$ are encouraged to be highly predictive of y at any p_{int} and for reasonable values of λ . Although not perceived there as strong evidence for leakage, a clear embedding structure based on the task label was also reported in Espinosa Zarlenga et al. (2022), Section 5.3.

Information theory offers additional insight into this phenomenon, in particular via the $\tilde{I}^{(CT)}(\hat{\mathbf{c}}^w, y)$ score defined in (10). As shown in Figure 10, qualitatively its values across models are representative of the degree of refinement in the structure of learnt embeddings displayed in Figures 9 and 25, and furthermore they closely track task accuracy. On the other hand, concept accuracy does not correlate with task accuracy or $\tilde{I}^{(CT)}$. This not only indicates the presence of concepts-task leakage, but also suggests that CEMs heavily rely on concepts-task leakage for task predictions: regardless of concepts, task accuracy is higher in models where the vectors $\hat{\mathbf{c}}_i^w$ encode more information about y .

The general dependence of CEMs on leaked information is further substantiated by the fact that task accuracy is insensitive to the number of used concepts, as demonstrated in the experiments reported in Espinosa Zarlenga et al. (2022), Appendix 8. When training CEMs on the CUB dataset with up to 90% of the annotated concepts removed, the task accuracy remains essentially the same as that of models trained on all the concepts. Along the same lines, the rigorous analysis carried out in Espinosa Zarlenga et al. (2022) using the information bottleneck paradigm evidences that in CEMs there is no information bottleneck and that information can freely flow from the input to the task prediction. Initially misunderstood, this result stands as a fundamental proof that the high-dimensional concept representations $\hat{\mathbf{c}}_i^w$ generally encode an arbitrary amount of information about the task, meeting the only requirement of being predictive of the real-valued concepts c_i .

Finally, in Appendix I we report on the subtle effect of *alignment leakage*, a subtype of concepts-task leakage that may generally appear in models such as CEMs which are exposed to interventions during training. We find evidence of this effect in experiments on

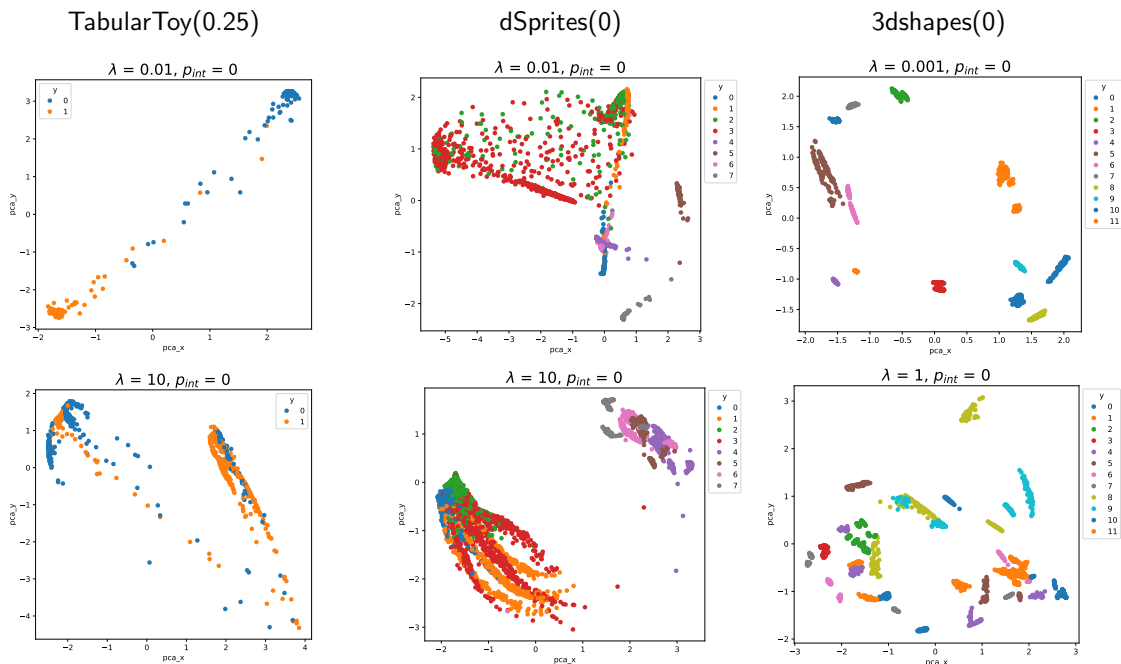


Figure 9: 2-dimensional PCA projections of the weighted embeddings $\hat{\mathbf{c}}_1^w$ for the first concept across datasets and for different values of λ at $p_{int} = 0$. The colouring indicates the value of the ground-truth task label.

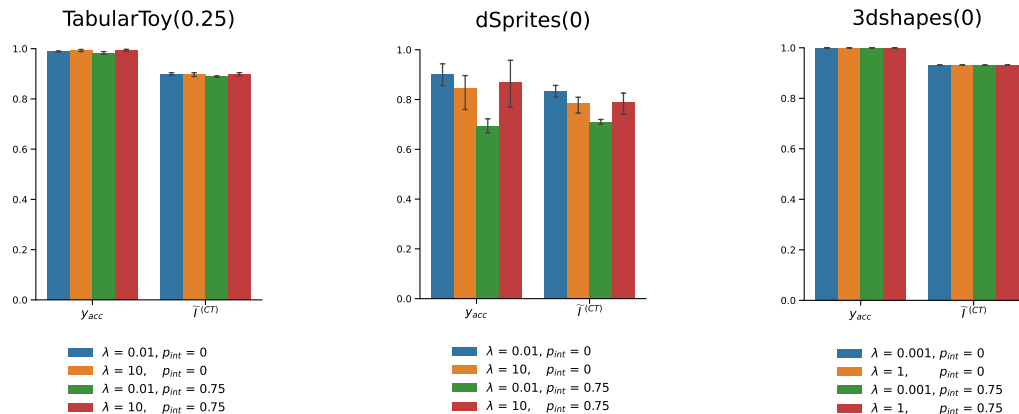


Figure 10: Task accuracy and $\tilde{I}^{(CT)}$ score on a range of CEMs and datasets.

the TabularToy(δ) dataset. Alignment leakage appears to be stronger in CEMs with higher λ and p_{int} , supporting its relation with exposure to intervention at training time.

Interconcept leakage increases with stronger concept supervision. Upon closer inspection of the structure of the learned embeddings $\hat{\mathbf{c}}_i^w$, significant clustering is also observed based on the ground-truth values of the other concepts $j \neq i$. This is evidenced in Figure 11, where we display the PCA projections of $\hat{\mathbf{c}}_1^w$ in terms of the values of c_2 and c_3

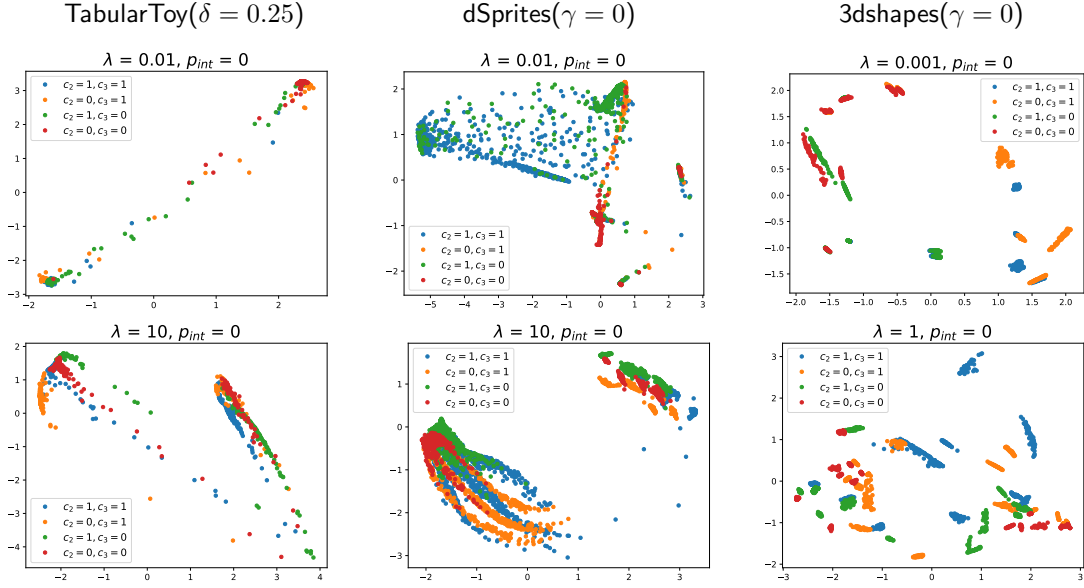


Figure 11: 2-dimensional PCA projections of the weighted embeddings \hat{c}_1^w for the first concept across datasets and for different values of λ at $p_{int} = 0$. The colouring indicates the ground-truth value of concepts 2 and 3.

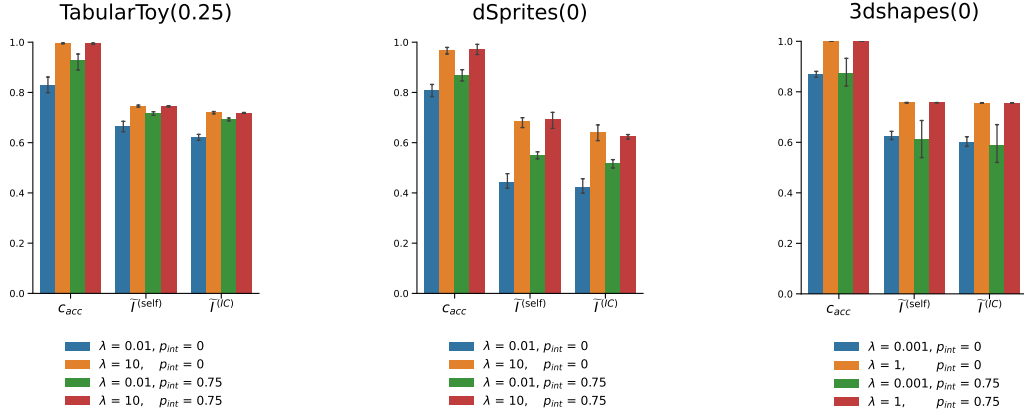


Figure 12: Concept accuracy as well as $\tilde{I}^{(IC)}$ and $\tilde{I}^{(\text{self})}$ scores for CEMs with low and high λ and p_{int} .

(see Figure 26 for similar plots for models with non-vanishing p_{int}). As especially manifest in TabularToy(0.25), where the task is binary and there is a total of three concepts, the fine structure present in Figures 9 and 25 which is not explained by the y labels is descriptive of the value of the other concepts.

This can be appreciated more quantitatively using the information-theoretic measures $\tilde{I}^{(IC)}(\hat{c}^w, c)$ and $\tilde{I}^{(\text{self})}(\hat{c}^w, c)$ defined in equations (11)-(12). As indicated in Figure 12 by higher c_{acc} and $\tilde{I}^{(\text{self})}$, each vector \hat{c}_i^w becomes more and more predictive of the corresponding c_i as one increases λ and p_{int} . This is the expected and desired behaviour as

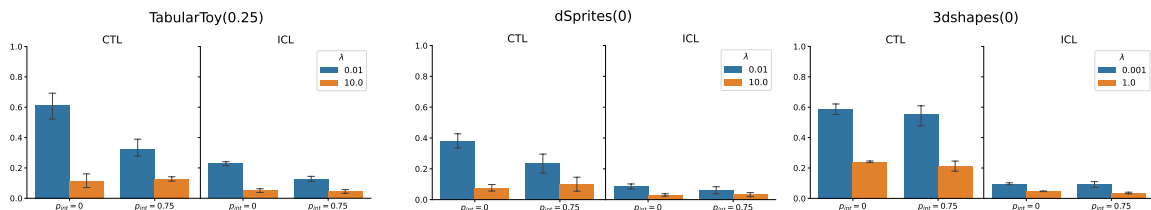


Figure 13: CTL and ICL scores evaluated on the predicted concept probabilities \hat{c}_i in CEMs with different λ and p_{int} .

it corresponds to increasing concept supervision. However, $\tilde{I}^{(IC)}$ undergoes a very similar growth, entailing that the vectors $\hat{\mathbf{c}}_i^w$ contain more and more information about the other concepts. By definition, this represents interconcept leakage.³ In contrast to CBMs, there is no choice of the hyperparameters λ and p_{int} that improves concept learning while decreasing interconcept leakage. Although again misinterpreted at the time, concept embeddings were found to be very predictive of the value of the other concepts also in Espinosa Zarlenga et al. (2022), Appendix 9.

To gain deeper insight into this interconcept leakage in CEMs, we evaluate the CTL and ICL scores on the predicted concept probabilities \hat{c}_i . Although not indicative of model interpretability – since reasoning occurs at the level of the weighted vectors – it is worth noting that they decrease in a manner similar to CBMs as concept supervision increases. The picture that emerges is thus that as one raises λ and p_{int} , the leaked information vanishes from the concept probabilities, and is effectively transferred into the vector representations as interconcept leakage. Vector representations in CEMs hence provide a mechanism for interconcept leakage to persist even at high concept supervision.

9 Lessons for model design

Our results on leakage enable us to outline the key steps for designing and training a concept-based model to ensure its interpretability. The first step consists of assessing whether the annotated concepts are sufficiently predictive of the task. To that aim, one should train several classifier heads on the ground-truth concepts, starting from a linear baseline. Depending on the use-case, while the choice of an interpretable head (such as a linear classifier) may be desirable, it may also result in severe misspecification. In this case, one should expect the gain in functional interpretability to be compensated to a certain extent by higher leakage, as per the results of Section 7.

If a sufficiently high task accuracy is not achieved with arbitrarily complex architectures, this is generally an indication that the set of concepts is not complete for the task. This either causes a drop in task performance in the case of hard architectures, or introduces a significant amount of leakage in the case of soft architectures. Furthermore, the experiments from Section 7 suggest that higher concept supervision is not sufficient in general to prevent leakage in such cases. If additional annotated concepts are not available, one should thus

3. For this experiment, we deliberately selected datasets where ground-truth interconcept MIs are minimal or vanishing. As a result, there is no interconcept structure for models to learn, nor any justification for concept representations to be highly predictive of the other concepts.

conclude that the task is not amenable to a concept-based approach given the dataset at hand.

Possible solutions to concept set incompleteness have been studied, including adding unsupervised concepts or channels, meant to account for the missing information (see Mahinpei et al., 2021; Havasi et al., 2022; Sawada and Nakamura, 2022; Yuksekgonul et al., 2023; Sheth and Kahou, 2023; Ismail et al., 2024, 2025). However, when adopting this approach, one has to ensure the model does not over-rely on such unsupervised channels, effectively bypassing the concept bottleneck when making a task prediction. Especially for high-risk scenarios, a general framework to interpret unknown concepts and safely include them in the concept refinement process is still missing.

It is also worth noting that an incomplete concept set and a misspecified classifier head are in principle degenerate issues, both leading to a drop in task performance and similarly higher leakage scores. Quantifying the completeness of a concept set for a given task is by itself an information-theoretic problem that has been extensively discussed in the context of feature selection, and measures have been presented e.g. in Yeh et al. (2020); Havasi et al. (2022), which may provide indications to break such a degeneracy.

If such issues do not arise, concept-based models can be adopted. The results of Section 7 highlight that concept encoding is a crucial aspect of model design, and should not be overly expressive relative to the type of annotated concepts to prevent leakage. Logit encoding is over-expressive for binary concepts, while it is arguably a suitable choice for continuous concepts. Similarly, vector encoding may be generally over-expressive for one-dimensional variables.

For binary annotated concepts, two common setups are soft and hard CBMs. To reduce leakage and achieve accurate concept learning, soft CBMs should be trained at relatively high $\lambda \in (\lambda_{min}, \lambda_{max})$, according to the results of Section 7. The *CTL* and *ICL* scores enable tuning λ to values that minimise leakage. Throughout our experiments they also evidenced that leakage is generally non-vanishing in soft CBMs. This may be acceptable depending on the use case, particularly since at high λ the model’s reliance on leaked information may be secondary to concept activations. Evaluating task performance on a number of soft and hard models, we also observe that soft CBMs with high λ are typically superior to hard CBMs in terms of task performance only in the cases where the classifier head is misspecified, while being essentially comparable in the other cases (Table 4). Note that when designing a concept-based model, it can be beneficial to also train an end-to-end black-box model without concept supervision, in order to establish an upper bound on the overall task performance and to assess the intrinsic predictivity of the input data for the task.

The results of this work support the information-theoretic framework that we propose as a novel and fundamental paradigm for assessing the interpretability of concept-based models. The leakage measures we introduce are robust and sensitive, and we advocate for their adoption as standard tools for ensuring interpretability when designing concept-based models.

Acknowledgments and Disclosure of Funding

y_{acc}	Soft	Hard
TT(0.25)	0.988 ± 0.004	0.990 ± 0.003
TT(0.25) incomplete	0.799 ± 0.008	0.787 ± 0.001
TT(0.25) misspecified	0.776 ± 0.030	0.713 ± 0.001
TT(0.75)	0.970 ± 0.033	0.975 ± 0.015
dS(0)	0.935 ± 0.017	0.944 ± 0.011
dS(0) incomplete	0.682 ± 0.016	0.701 ± 0.010
dS(0) misspecified	0.983 ± 0.002	0.928 ± 0.012
dS(4)	0.941 ± 0.013	0.953 ± 0.012
3ds(0)	1.000 ± 0.000	1.000 ± 0.000
3ds(0) incomplete	0.675 ± 0.048	0.653 ± 0.001
3ds(0) misspecified	0.998 ± 0.005	0.854 ± 0.007
3ds(5)	1.000 ± 0.000	1.000 ± 0.000

Table 4: Task accuracies of soft and hard CBMs trained for the experiments in Section 7. The soft models are trained with $\lambda = 10$ for TabularToy and dSprites, and with $\lambda = 1$ for 3dshapes.

We thank Aya Abdelsalam Ismail, Anthony Baptista and Gregory Verghese for insightful discussions on related topics. All authors except CH are supported by the Turing-Roche strategic partnership. CRSB is supported by the CRUK City of London Centre Award [CTRQQR-2021\100004]. TC is supported by a principal research fellowship from University College London.

Appendix A. Details on the experimental setup

A.1 Datasets

For additional details on these datasets, we refer the reader to .

TabularToy(δ). This dataset is constructed by sampling a 3-dimensional latent variable $z \sim \mathcal{N}(0, \Sigma(\delta))$, with correlation matrix $\Sigma(\delta)_{ij} = \delta_{ij} + \delta(1 - \delta_{ij})$ with $i, j = 1, 2, 3$, δ_{ij} Kronecker symbol and $\delta \in (-1, 1)$ indicating the correlation between components. The 7-dimensional input x is a trigonometric function of the latent variables (see Mahinpei et al., 2021), while the three binary concepts are defined as the sign of the latent variables, $c_i = (z_i > 0)$. The binary task label is the following linear function of concepts,

$$y_{\text{TT}}^{(orig)} = (c_1 + c_2 + c_3 \geq 2). \quad (13)$$

For our experiments we generate a dataset of size 10K, with a 0.7/0.2/0.1 train / validation / test ratio. For Figures 2 and 3 we consider a simplified version of TabularToy(δ) with only the first two concepts c_1 and c_2 for each input, and binary task $y = (c_1 + c_2 \geq 1)$.

dSprites(γ). For this family of datasets, each input $x \in \{0, 1\}^{64 \times 64 \times 1}$ is an image generated deterministically from five latent variables $z = (\text{shape} \in \{0, 1, 2\}, \text{scale} \in \{0, \dots, 5\}, \theta \in \{0, \dots, 39\}, X \in \{0, \dots, 31\}, Y \in \{0, \dots, 31\})$, where shape corresponds to either a square, ellipse or a heart, while θ , X and Y indicate the rotation and the position of

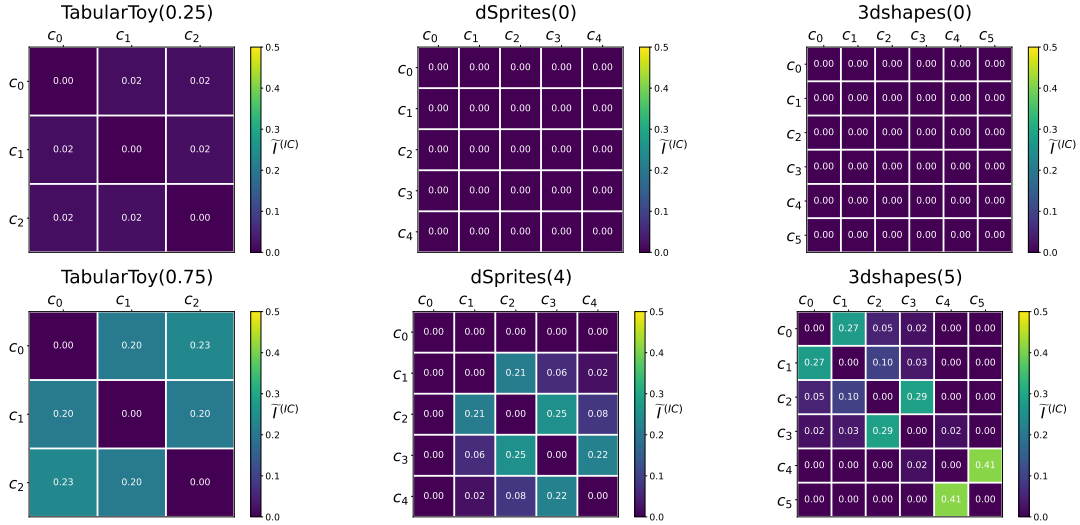


Figure 14: Ground-truth interconcept normalised MI in the used datasets.

the shape in the plane respectively. Following Espinosa Zarlenga et al. (2023a), we define dSprites(0) as the datasets with no interconcept correlations. Here the five binary concepts are based on the value of the latent variables, $c = (z_1 < 2, z_2 < 3, z_3 < 20, z_4 < 16, z_5 < 16)$, and the 8-class task label is

$$y_{\text{ds}}^{(\text{orig})} = (1 - c_1)(2c_4 + c_5 + 4) + c_1(2c_2 + c_3). \quad (14)$$

To generate dSprites(γ) with increasing interconcept correlations for $\gamma = 1, \dots, 4$, we adopt the procedure detailed in Espinosa Zarlenga et al. (2023a). We use datasets with approximately 25K and 14K samples for dSprites(0) and dSprites(4) respectively, with a 0.75/0.25 train / test ratio.

3dshapes(γ). Each input is an image $x \in \{0, 1\}^{64 \times 64 \times 3}$ generated from six latent variables $z = (\text{floor_hue} \in \{0, \dots, 9\}, \text{wall_hue} \in \{0, \dots, 9\}, \text{object_hue} \in \{0, \dots, 9\}, \text{scale} \in \{0, \dots, 7\}, \text{shape} \in \{0, 1, 2, 3\}, \text{orientation} \in \{0, \dots, 14\})$, where shape denotes either a sphere, a cube, a capsule or a cylinder. Following Espinosa Zarlenga et al. (2023a), in 3dshapes(0) concepts are defined as $c = (z_1 < 5, z_2 < 5, z_3 < 5, z_4 < 4, z_5 < 2, z_6 < 7)$, and the 12 class labels are obtained as

$$y_{\text{3ds}}^{(\text{orig})} = (1 - c_5)(2c_1 + c_2) + c_5(4c_3 + 2c_4 + c_6 + 4) \quad (15)$$

Increasing interconcept correlations are induced for $\gamma = 1, \dots, 5$ in a similar fashion to dSprites(γ). For our experiments we consider 3dshapes(0) and 3dshapes(5) with size 16K and 14K respectively, and a 0.7/0.1/0.2 train / validation / test ratio.

Ground-truth interconcept correlations. In Figure 14 we display as a reference the ground-truth interconcept normalised MI for the training datasets used in the experiments.

Experiments with incomplete concept set. In TabularToy(0.25), we remove c_3 from the three concepts. In dSprites(0), we remove c_4 and c_5 from the five concepts. In 3dshapes(0), we remove c_3 and c_6 from the six concepts.

Experiments with misspecified head. We provide here more details on the experiments to assess the effects of a misspecified final head discussed in Section 7. To generate non-linear concepts-task dependences in $\text{TabularToy}(\delta)$, we add a non-linear term to the original linear task in (13), resulting in the binary classification problem,

$$y_{\text{TT}}^{(new)} = (c_1 + c_2 + c_3 - c_1c_2 \geq 2).$$

The original tasks in (14) and (15) for $\text{dSprites}(\gamma)$ and $\text{3dshapes}(\gamma)$ are non-linear, however a linear classifier is able to reach essentially perfect task accuracy (Table 3). To induce a sizeable misspecification, we thus add further higher-order non-linear terms. The tasks implemented for our experiments on $\text{dSprites}(0)$ and $\text{3dshapes}(0)$ read,

$$\begin{aligned} y_{\text{dS}}^{(new)} &= y_{\text{dS}}^{(orig)} - (1 - c_1)c_3c_4 - c_1(c_2c_5 + c_3c_5 + c_2c_4), \\ y_{\text{3ds}}^{(new)} &= y_{\text{3ds}}^{(orig)} - 3c_1c_2c_3 - c_4c_5c_6 - c_1c_3c_5 + c_2c_4c_6. \end{aligned}$$

A.2 Model architectures and training

On $\text{TabularToy}(\delta)$ we use as concept encoder a 4-layer leaky-ReLU MLP with activations $\{7, 64, 64, 3\}$, and a linear classifier head. On $\text{dSprites}(\gamma)$ and $\text{3dshapes}(\gamma)$ we use a ResNet-18 encoder, and a 4-layer ReLU MLP with activations $\{k, 64, 64, \ell\}$. We train CEMs with 16-dimensional embeddings.

We train all models for 200 epochs, using the Adam optimiser with learning rate 10^{-3} and momentum 0.9. For hard models, we train the encoder and the classifier head for 200 and 20 epochs respectively. We train with batch sizes 512 for $\text{TabularToy}(\delta)$ and 32 for $\text{dSprites}(\gamma)$ and $\text{3dshapes}(\gamma)$.

A.3 Scores evaluation

Except for Figure 14, all the displayed scores are evaluated on test sets. The reported intervention performances are obtained with a random policy. In Figures 3, 4 and 16 we show results for single models, and the displayed means and 95% confidence intervals refer to a 5-fold evaluation of each score. In the rest of the paper, we repeat the evaluation of each score 5 times for individual models, and we display means and 95% confidence intervals representing the distribution of the mean upon 5-fold training for each model class. MIs and entropies are estimated via the KSG estimator (Kraskov et al., 2004) with 3 nearest neighbours. The OIS and NIS are evaluated using their original implementations and default settings from Espinosa Zarlenga et al. (2023a).

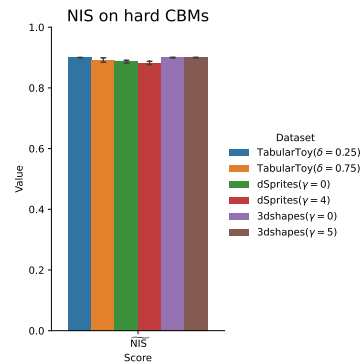


Figure 15: $\widetilde{\text{NIS}}$ evaluated on hard CBMs across datasets.

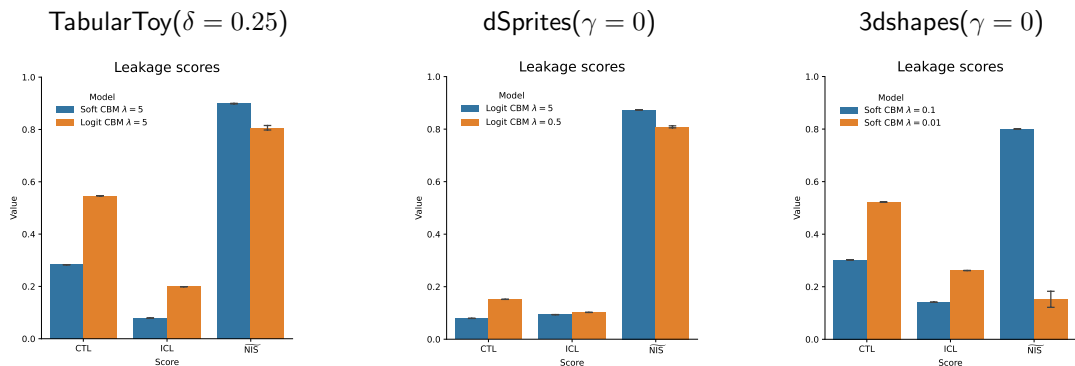


Figure 16: $\widetilde{\text{NIS}}$ and leakage scores for the pairs of models assessed in Figure 4, Table 1.

Appendix B. Undesired features of the Niche Impurity Score

Being computed as an AUC, $\text{NIS} = 1/2$ indicates that concept representation subsets are not predictive of the value of concepts, while $\text{NIS} = 1$ is meant to indicate that the higher-order interconcept leakage is maximal. For a fair comparison of our scores with NIS, we plot $\widetilde{\text{NIS}} = 2(\text{NIS} - 1/2)$, taking values in $(0, 1)$ corresponding to no and maximal leakage respectively.

Evaluating NIS on the pairs of models considered in Figure 4, this score appears to be anticorrelated with intervention performance and leakage (Figure 16). Furthermore, it takes proportionally very high values regardless of the model and dataset. This is confirmed by its behaviour on hard CBMs (Figure 15): the NIS is non-vanishing and very high in all cases. These undesired features that NIS generally exhibits signal potential flaws in its design and make it an unsuitable metric of leakage.

Appendix C. Concept-wise leakage scores

The concept-wise leakage scores defined in (6) and (9) provide more granular information on the leakage encoded in each concept. In Figure 17 we display the CTL_i and ICL_i scores for the pairs of models analysed in Figure 4 and Table 1. Note in particular that i) leakage is not necessarily learnt homogeneously across concepts, and ii) comparing two models with different levels of interpretability, certain concepts may exhibit comparable amounts of leakage (such as c_4 in the dSprites(0) example), while for others leakage may be significantly different. Concept-wise scores are sensitive to both phenomena, making them valuable indicators of per-concept risk upon intervention as well as important measures for model design.

Appendix D. Details on the correlation between leakage scores and intervention performance

The models considered for this computation are

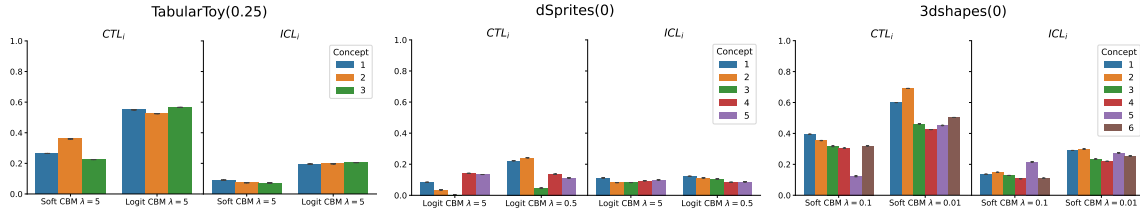


Figure 17: Concept-wise leakage scores evaluated on the pairs of models in Figure 4.

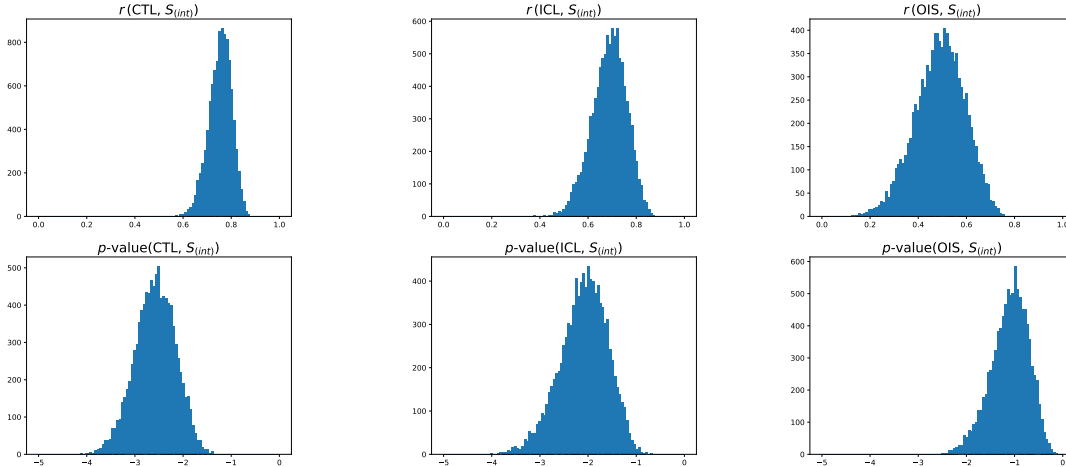


Figure 18: Distributions of Pearson r and corresponding p -values between the intervention score $S_{(int)}$ and the CTL, ICL and OIS leakage metrics for TabularToy(0.25).

- for the TabularToy(0.25), TabularToy(0.75), dSprites(0), dSprites(4) datasets: soft and logit CBMs with $\lambda = 0.01, 0.1, 0.5, 1, 5, 10$;
- for the 3dshapes(0), 3dshapes(5) datasets: soft and logit CBMs with $\lambda = 0.001, 0.005, 0.01, 0.05, 0.1, 0.5, 1$.

Each class of models were trained over 5 folds, amounting to a total of 60 evaluated models for each of the former four datasets, and to a total of 70 models for each of the latter two datasets.

As an example, in Figure 18 we display the distributions of the Pearson r and p -values between intervention performance and the CTL, ICL, OIS scores resulting from MC-sampling for the TabularToy(0.25) dataset.

Appendix E. Behaviour of CBMs at high λ

In soft and logit CBMs leakage is minimal for values of $\lambda > \lambda_{min}$, where λ_{min} is specific of the considered model class (Figure 19). As one further increases λ , leakage scores remain essentially constant. At significantly higher $\lambda \gtrsim \lambda_{max}$ concept supervision may however become too strong, at the expense of task learning. In such cases,

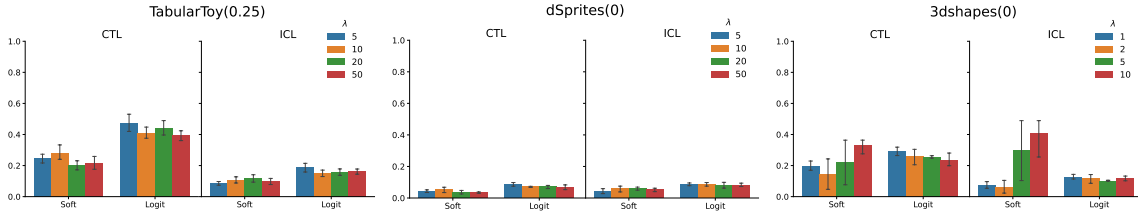


Figure 19: Leakage scores evaluated on soft and logit CBMs at high λ .

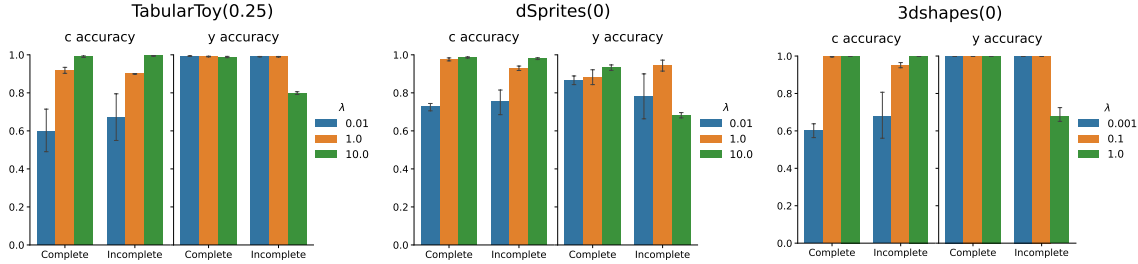


Figure 20: Concepts and task accuracies evaluated for the same models analysed in Figure 7 on datasets with complete and incomplete sets of concepts.

1. task performance may experience a drop. For instance, models trained on TabularToy(0.25) reach a task accuracy above 90% in only 3 out of 5 folds for each $\lambda = 10, 20, 50$;
2. leakage may raise again well above the minimal value. The soft models trained on 3dshapes(0) are a compelling example of this.

Finally, note that the minimal attainable leakage in logit CBMs is higher than in soft CBMs on a given dataset.

Appendix F. Performance of models with incomplete concept sets and misspecified head

In Figure 20 we report the task and concept accuracies of the soft CBMs trained on complete and incomplete sets of concepts discussed in Section 7. Note in particular the decrease in task accuracy at high λ that manifests in case of incomplete concept sets. At low λ , leakage is sufficient to ensure task accuracy remains essentially the same as in the case of complete concept sets. Figure 21 presents the task and concept accuracies of the well-specified and misspecified soft CBMs evaluated in Figure 8 and discussed in Section 7.

Appendix G. Dimensional-dependent bias in MI estimators

MI estimators are affected by significant biases in high dimensions as a general consequence of the curse of dimensionality (Lord et al., 2018; Carrara and Ernst, 2019; Czyż et al., 2023; Gowri et al., 2024). This results in MI estimates that cannot be compared across dimensions, as such biases are dimension-dependent. To illustrate this issue for the KSG estimator we

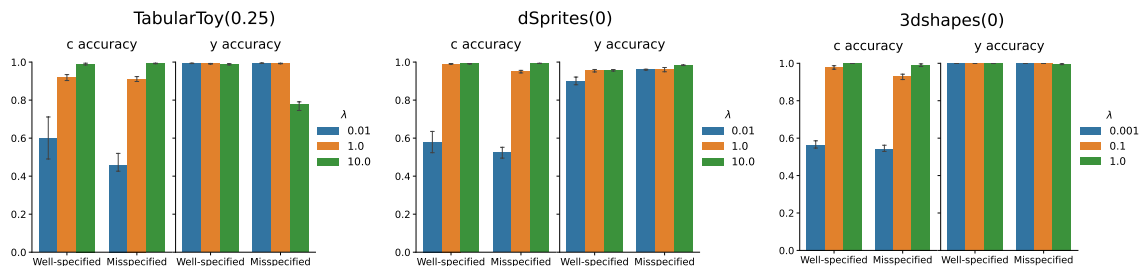


Figure 21: Concepts and task accuracies evaluated for the same models with a linear head analysed in Figure 8 trained on datasets with linear and non-linear tasks as functions of concepts.

adopt in this work, we consider normally-distributed higher-dimensional variables with non-trivial correlations, for which MIs and entropies can be computed in closed form. To see the effect of the dimension on the normalised interconcept MI, we sample two d -dimensional random variables $(X, Y) \sim \mathcal{N}(0, \Sigma^{(IC)}(\rho))$, where the covariance takes the form, $\Sigma^{(IC)} = \begin{pmatrix} \mathbf{I}_d & \rho \mathbf{I}_d \\ \rho \mathbf{I}_d & \mathbf{I}_d \end{pmatrix}$, where \mathbf{I}_d denotes the identity matrix of dimension d , and $\rho \in (-1, 1)$ measures the linear correlation between each component of X and Y . To model concepts-task MI, we consider two variables $X \in \mathbb{R}^d$ and $Y \in \mathbb{R}$ drawn from a normal distribution with zero mean and covariance matrix

$$\Sigma^{(CT)} = \begin{pmatrix} 1 & \cdots & 0 & \rho \\ \vdots & \ddots & \vdots & \vdots \\ 0 & \cdots & 1 & \rho \\ \rho & \cdots & \rho & 1 \end{pmatrix}, \quad (16)$$

where all the components of X are equally correlated with Y . Note that $\Sigma^{(CT)}$ is positive-definite only for $0 \leq \rho < 1/\sqrt{d}$, hence we will consider covariances only within this range.

For normally-distributed variables, entropy and MI can be computed in closed form (Cover and Thomas, 2005). Considering two variables $(X, Y) \sim \mathcal{N}(\mu, \Sigma)$ of dimensions d_X and d_Y respectively, and $\Sigma^{(IC)} = \begin{pmatrix} \Sigma_X & \tilde{\Sigma} \\ \tilde{\Sigma} & \Sigma_Y \end{pmatrix}$, the entropy and MI read,

$$H(X) = \frac{d_X}{2} (1 + \log 2\pi), \quad I(X, Y) = \frac{1}{2} \log \frac{|\Sigma_X| |\Sigma_Y|}{|\Sigma|}, \quad (17)$$

where $|\cdot|$ denotes the determinant. For interconcept MI with $d_X = d_Y = d$, this entails the following theoretic values for MI and normalised MI,

$$I^{(IC)}(X, Y) = -\frac{d}{2} \log(1 - \rho^2), \quad \tilde{I}^{(IC)}(X, Y) = \frac{I^{(IC)}(X, Y)}{\sqrt{H(X)H(Y)}} = -\frac{\log(1 - \rho^2)}{1 + \log 2\pi}, \quad (18)$$

while for concepts-task MI with $d_X = d$ and $d_Y = 1$,

$$I^{(CT)}(X, Y) = -\frac{1}{2} \log(1 - d\rho^2), \quad \tilde{I}^{(CT)}(X, Y) = \frac{I^{(CT)}(X, Y)}{H(Y)} = -\frac{\log(1 - d\rho^2)}{1 + \log 2\pi}. \quad (19)$$

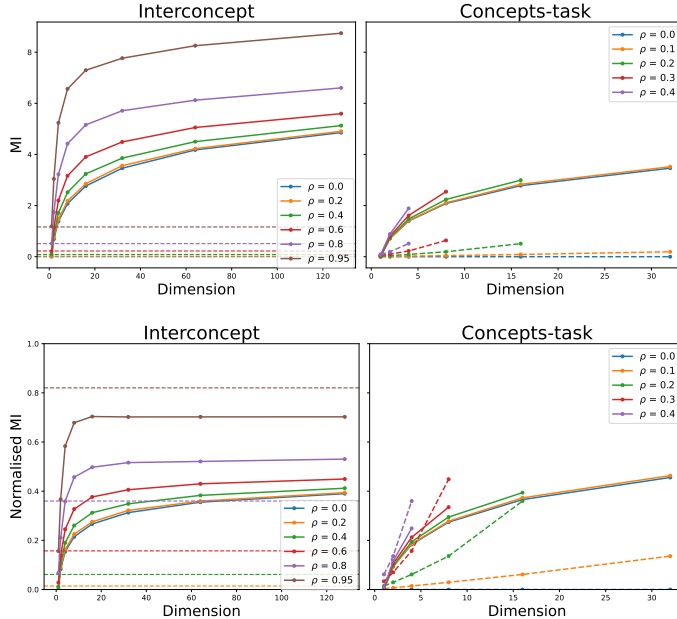


Figure 22: Results for the Gaussian experiment illustrating the bias in estimates of MI and normalised MI depending on the dimension and covariance.

We compare these predicted behaviours with the MIs and normalised MIs obtained with the KSG estimator (Kraskov et al., 2004) on a range of correlations and dimensions. The results are displayed in Figure 22, where the theoretic behaviours for different ground-truth correlations are represented with dashed lines.

Although monotonically related to the theoretic values, the estimated normalised MIs are pushed towards higher and higher values as one increases the dimension, regardless of the ground-truth correlation. This prevents comparing quantities estimated on concept representations of different dimensions as required by the definitions of the CTL and ICL scores in (6)-(8), while still enabling one to compare MIs and normalised MIs for concept representations of the same dimension. Note also that these results cannot be used as calibration curves to account for such biases, since these Gaussian models only incorporate linear correlations, while leakage more generally manifests as shared information between two variables.

OIS is affected by the same type of biases. As discussed in Section 4, the OIS is meant to be a rough estimate of interconcept leakage, and hence of interconcept MI when ground-truth interconcept correlations are negligible. In Figure 23 we display the OIS scores for the 16-dimensional concept vector representations $\hat{\mathbf{c}}_i^w$ in a number of CEMs trained with different λ and p_{int} . We note OIS is generally very high and affected by the same biases as the standard MI estimators, casting further doubts on its utility for higher-dimensional concept representations.

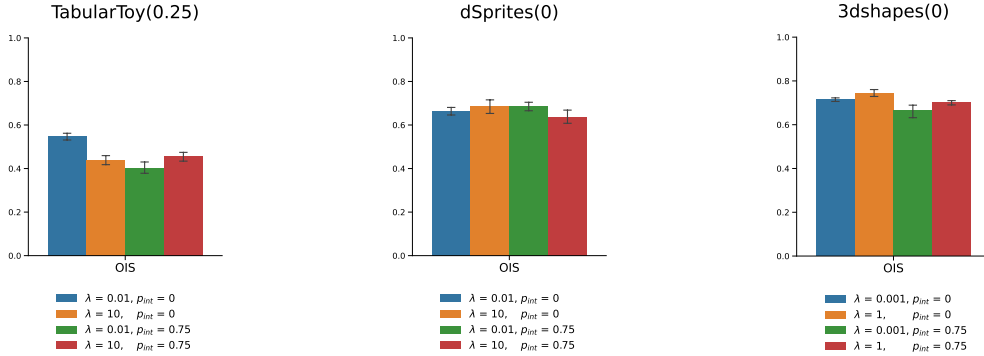


Figure 23: The OIS values computed on the vectors \hat{c}_i^w learnt by CEMs with low and high λ and p_{int} , on TabularToy(0.25), dSprites(0) and 3dshapes(0).

Appendix H. Further results on CEM non-interpretability

Embedding structure at non-vanishing p_{int} . In Figures 25 and 26 we display the PCA projections of the weighted vectors \hat{c}_1^w with colouring based on the ground-truth value of the task label and of concepts 2 and 3 respectively, at non-vanishing p_{int} and for low and high λ .

Concept accuracy and intervention performance are not measures of interpretability in CEMs. As demonstrated in Section 8, CEMs generally encode high amounts of concepts-task leakage, and from this perspective, concept accuracy is only a measure of how predictive the vectors \hat{c}_i^w are of concept i , fully unable to capture the additional information about the task that the embeddings encode. Furthermore, as shown in Figure 12, interconcept leakage increases as one raises concept supervision. Thus c_{acc} typically correlates with interconcept leakage in CEMs.

Intervention performance is not an indicator of leakage either – it is very high in models with severe leakage (Figure 27). In particular, CEMs where high concepts-task leakage is present in both \hat{c}_i^+ and \hat{c}_i^- are able to achieve a vanishing $S_{(int)}$. This motivates the definition and adoption of more sensitive information-theoretic measures for CEMs, such as (10), (11) and (12).

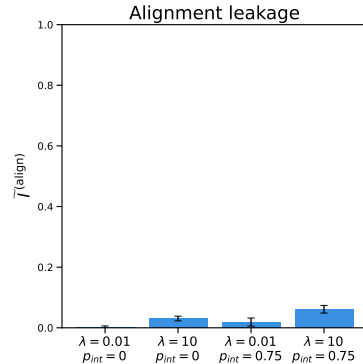


Figure 24: Alignment leakage score for CEMs trained on the TabularToy(0.25) dataset with low and high λ and p_{int} .

Appendix I. Alignment leakage in CEMs

A subtle leakage effect may in principle arise when exposing a model like CEMs to interventions during training. For each data point $n \in \{1, \dots, N\}$ with ground-truth value $c_i^{(n)}$ for concept i , we denote by aligned (unaligned) vector the one between $\hat{c}_i^{+(n)}$ or $\hat{c}_i^{-(n)}$ which

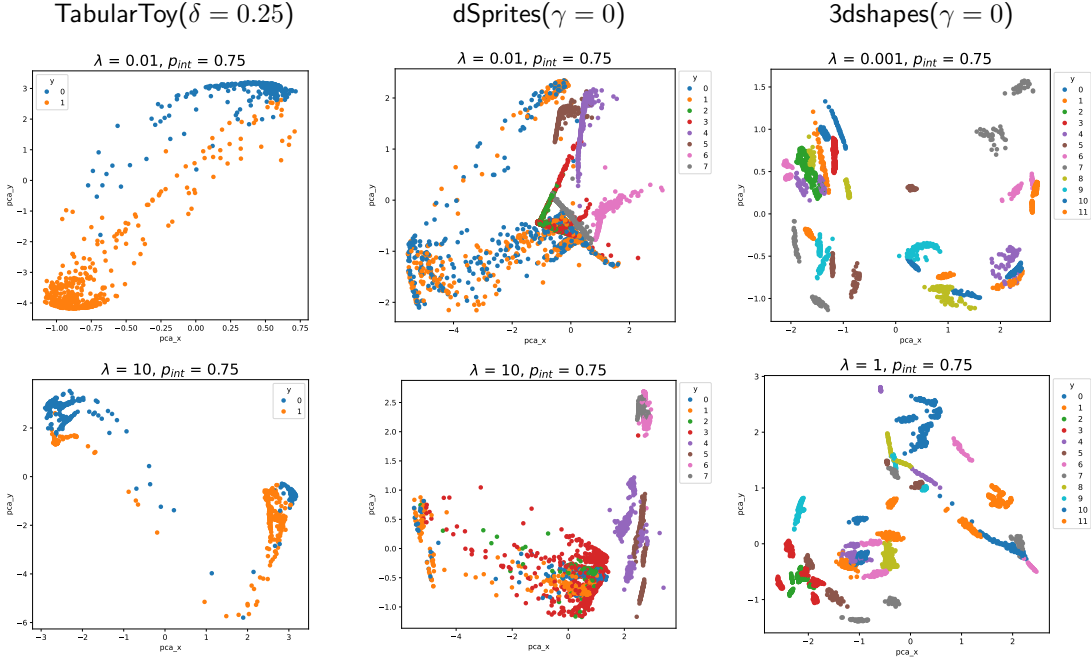


Figure 25: 2-dimensional PCA projections of the weighted embeddings \hat{c}_1^w for the first concept across datasets and for different values of λ at high $p_{int} = 0.75$. The colouring indicates the value of the ground-truth task label.

is aligned (unaligned) with the value of $c_i^{(n)}$: if $c_i^{(n)} = 1$, $\hat{c}_i^{+(n)}$ ($\hat{c}_i^{-(n)}$) is the aligned (unaligned) vector, and vice versa $\hat{c}_i^{-(n)}$ ($\hat{c}_i^{+(n)}$) is the aligned (unaligned) vector for $c_i^{(n)} = 0$. The meaning of this distinction is that after intervening on the i -th concept at training or test time, the weighted vector $\hat{c}_i^{w(n)}$ is equal to the aligned vector. A model exposed to interventions may thus learn to improve performance upon interventions by generating aligned vectors that are more predictive of the task than the unaligned ones. This form of leakage results in embeddings that have inhomogeneous reliability depending on the alignment with ground-truth concepts, leading to an overall reduction in model interpretability.

This effect, which we label *alignment leakage*, is a specific manifestation of concepts-task leakage. To quantify it, we define the following information-theoretic score, which indicates to what extent aligned vectors are more predictive of the task than unaligned vectors across both positive and negative embeddings, as an excess in concepts-task normalised MIs as defined in (10),

$$\begin{aligned} \tilde{I}^{(\text{align})}(\hat{c}^+, \hat{c}^-, c, y) &= \tilde{I}^{(CT)}(\hat{c}^{+(\text{aligned})}, y) - \tilde{I}^{(CT)}(\hat{c}^{+(\text{unaligned})}, y) \\ &+ \tilde{I}^{(CT)}(\hat{c}^{-(\text{aligned})}, y) - \tilde{I}^{(CT)}(\hat{c}^{-(\text{unaligned})}, y), \end{aligned} \quad (20)$$

where $\hat{c}^{\pm(\text{aligned})}$ denote the set of positive/negative vectors aligned with the corresponding ground-truth concept, and analogously for $\hat{c}^{\pm(\text{unaligned})}$. $\tilde{I}^{(\text{align})}$ takes values in $(-2, 2)$ in units of normalised MI; positive values indicate that the aligned vectors are more predictive of the task than the unaligned ones, while a value of zero corresponds to no alignment leakage.

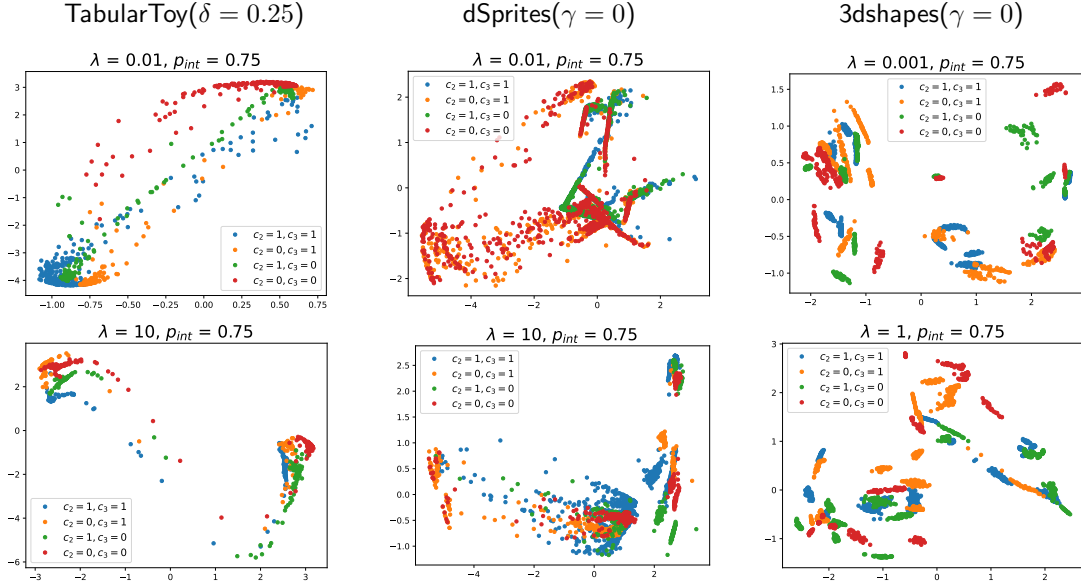


Figure 26: 2-dimensional PCA projections of the weighted embeddings \hat{c}_1^w for the first concept across datasets and for different values of λ at high $p_{int} = 0.75$. The colouring indicates the ground-truth value of concepts 2 and 3.

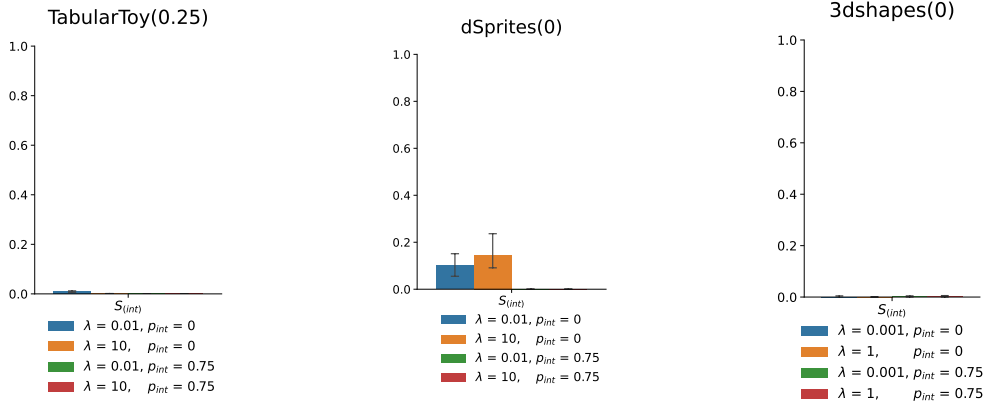


Figure 27: The $S_{(int)}$ score for CEMs with low and high λ and p_{int} .

We assess this form of leakage in CEMs trained at different values of λ and p_{int} . While in models trained on dSprites(0) and 3dshapes(0) it does not appear, we find $\tilde{I}^{(align)}$ scores incompatible with zero for models trained on TabularToy(0.25) (Figure 24). Alignment leakage is stronger in models at high λ and p_{int} , supporting the intuition that such a detrimental effect correlates with exposure to interventions during training.

References

- Christopher RS Banerji, Tapabrata Chakraborti, Aya Abdelsalam Ismail, Florian Ostmann, and Ben D MacArthur. Train clinical ai to reason like a team of doctors. *Nature*, 639 (8053):32–34, 2025.
- Chris Burgess and Hyunjik Kim. 3d shapes dataset. <https://github.com/deepmind/3dshapes-dataset/>, 2018.
- Nicholas Carrara and Jesse Ernst. On the estimation of mutual information. *Proceedings*, 33(1), 2019. ISSN 2504-3900. doi: 10.3390/proceedings2019033031. URL <https://www.mdpi.com/2504-3900/33/1/31>.
- Kushal Chauhan, Rishabh Tiwari, Jan Freyberg, Pradeep Shenoy, and Krishnamurthy Dvijotham. Interactive concept bottleneck models. In *Proceedings of the Thirty-Seventh AAAI Conference on Artificial Intelligence and Thirty-Fifth Conference on Innovative Applications of Artificial Intelligence and Thirteenth Symposium on Educational Advances in Artificial Intelligence*, AAAI’23/IAAI’23/EAAI’23. AAAI Press, 2023. ISBN 978-1-57735-880-0. doi: 10.1609/aaai.v37i5.25736. URL <https://doi.org/10.1609/aaai.v37i5.25736>.
- T. M. Cover and J. A. Thomas. *Elements of Information Theory*. John Wiley & Sons, Ltd, 2005.
- Paweł Czyż, Frederic Grabowski, Julia E Vogt, Niko Beerenwinkel, and Alexander Marx. Beyond normal: On the evaluation of mutual information estimators. In *Thirty-seventh Conference on Neural Information Processing Systems*, 2023. URL <https://openreview.net/forum?id=25vRtG56YH>.
- Mateo Espinosa Zarlenga, Pietro Barbiero, Gabriele Ciravegna, Giuseppe Marra, Francesco Giannini, Michelangelo Diligenti, Zohreh Shams, Frederic Precioso, Stefano Melacci, Adrian Weller, Pietro Lio, and Mateja Jamnik. Concept embedding models: beyond the accuracy-explainability trade-off. In *Proceedings of the 36th International Conference on Neural Information Processing Systems*, NIPS ’22, Red Hook, NY, USA, 2022. Curran Associates Inc. ISBN 9781713871088.
- Mateo Espinosa Zarlenga, Pietro Barbiero, Zohreh Shams, Dmitry Kazhdan, Umang Bhatt, Adrian Weller, and Mateja Jamnik. Towards robust metrics for concept representation evaluation. *Proceedings of the AAAI Conference on Artificial Intelligence*, 37(10): 11791–11799, June 2023a. ISSN 2159-5399. doi: 10.1609/aaai.v37i10.26392. URL <http://dx.doi.org/10.1609/aaai.v37i10.26392>.
- Mateo Espinosa Zarlenga, Katie Collins, Krishnamurthy Dvijotham, Adrian Weller, Zohreh Shams, and Mateja Jamnik. Learning to receive help: Intervention-aware concept embedding models. In A. Oh, T. Naumann, A. Globerson, K. Saenko, M. Hardt, and S. Levine, editors, *Advances in Neural Information Processing Systems*, volume 36, pages 37849–37875. Curran Associates, Inc., 2023b. URL https://proceedings.neurips.cc/paper_files/paper/2023/file/770cabd044c4eacb6dc5924d9a686dce-Paper-Conference.pdf.

- Yibo Gao, Zheyao Gao, Xin Gao, Yuanye Liu, Bomin Wang, and Xiahai Zhuang. Evidential concept embedding models: Towards reliable concept explanations for skin disease diagnosis. In Marius George Linguraru, Qi Dou, Aasa Feragen, Stamatia Giannarou, Ben Glocker, Karim Lekadir, and Julia A. Schnabel, editors, *Medical Image Computing and Computer Assisted Intervention – MICCAI 2024*, pages 308–317, Cham, 2024. Springer Nature Switzerland. ISBN 978-3-031-72117-5.
- Gokul Gowri, Xiaokang Lun, Allon M Klein, and Peng Yin. Approximating mutual information of high-dimensional variables using learned representations. In *The Thirty-eighth Annual Conference on Neural Information Processing Systems*, 2024. URL <https://openreview.net/forum?id=HN05DQxyL1>.
- Marton Havasi, Sonali Parbhoo, and Finale Doshi-Velez. Addressing leakage in concept bottleneck models. In S. Koyejo, S. Mohamed, A. Agarwal, D. Belgrave, K. Cho, and A. Oh, editors, *Advances in Neural Information Processing Systems*, volume 35, pages 23386–23397. Curran Associates, Inc., 2022. URL https://proceedings.neurips.cc/paper_files/paper/2022/file/944ecf65a46feb578a43abfd5cddd960-Paper-Conference.pdf.
- Lijie Hu, Tianhao Huang, Huanyi Xie, Chenyang Ren, Zhengyu Hu, Lu Yu, and Di Wang. Semi-supervised concept bottleneck models. *ArXiv*, abs/2406.18992, 2024. URL <https://api.semanticscholar.org/CorpusID:270765040>.
- Qihan Huang, Jie Song, Jingwen Hu, Haofei Zhang, Yong Wang, and Mingli Song. On the concept trustworthiness in concept bottleneck models. In *Proceedings of the Thirty-Eighth AAAI Conference on Artificial Intelligence and Thirty-Sixth Conference on Innovative Applications of Artificial Intelligence and Fourteenth Symposium on Educational Advances in Artificial Intelligence, AAAI’24/IAAI’24/EAAI’24*. AAAI Press, 2024. ISBN 978-1-57735-887-9. doi: 10.1609/aaai.v38i19.30109. URL <https://doi.org/10.1609/aaai.v38i19.30109>.
- Aya Abdelsalam Ismail, Julius Adebayo, Hector Corrada Bravo, Stephen Ra, and Kyunghyun Cho. Concept bottleneck generative models. In *The Twelfth International Conference on Learning Representations*, 2024. URL <https://openreview.net/forum?id=L9U5MJJleF>.
- Aya Abdelsalam Ismail, Tuomas Oikarinen, Amy Wang, Julius Adebayo, Samuel Don Stanton, Hector Corrada Bravo, Kyunghyun Cho, and Nathan C. Frey. Concept bottleneck language models for protein design. In *The Thirteenth International Conference on Learning Representations*, 2025. URL <https://openreview.net/forum?id=Yt9CFh00Fe>.
- Dmitry Kazhdan, B. Dimanov, Helena Andrés-Terré, Mateja Jamnik, Pietro Lio’, and Adrian Weller. Is disentanglement all you need? comparing concept-based & disentanglement approaches. *CoRR*, abs/2104.06917, 2021.
- Eunji Kim, Dahuin Jung, Sangha Park, Siwon Kim, and Sungroh Yoon. Probabilistic concept bottleneck models. In *Proceedings of the 40th International Conference on Machine Learning, ICML’23*. JMLR.org, 2023.

- Sangwon Kim, Dasom Ahn, Byoung Chul Ko, In-su Jang, and Kwang-Ju Kim. Eq-cbm: A probabilistic concept bottleneck with energy-based models and quantized vectors. In Minsu Cho, Ivan Laptev, Du Tran, Angela Yao, and Hongbin Zha, editors, *Computer Vision – ACCV 2024*, pages 270–286, Singapore, 2025. Springer Nature Singapore. ISBN 978-981-96-0963-5.
- Pang Wei Koh, Thao Nguyen, Yew Siang Tang, Stephen Mussmann, Emma Pierson, Been Kim, and Percy Liang. Concept bottleneck models. In Hal Daumé III and Aarti Singh, editors, *Proceedings of the 37th International Conference on Machine Learning*, volume 119 of *Proceedings of Machine Learning Research*, pages 5338–5348. PMLR, 13–18 Jul 2020. URL <https://proceedings.mlr.press/v119/koh20a.html>.
- Alexander Kraskov, Harald Stögbauer, and Peter Grassberger. Estimating mutual information. *Phys. Rev. E*, 69:066138, Jun 2004. doi: 10.1103/PhysRevE.69.066138. URL <https://link.aps.org/doi/10.1103/PhysRevE.69.066138>.
- Neeraj Kumar, Alexander C. Berg, Peter N. Belhumeur, and Shree K. Nayar. Attribute and simile classifiers for face verification. In *2009 IEEE 12th International Conference on Computer Vision*, pages 365–372, 2009. doi: 10.1109/ICCV.2009.5459250.
- Christoph H. Lampert, Hannes Nickisch, and Stefan Harmeling. Learning to detect unseen object classes by between-class attribute transfer. In *2009 IEEE Conference on Computer Vision and Pattern Recognition*, pages 951–958, 2009. doi: 10.1109/CVPR.2009.5206594.
- Joshua Lockhart, Nicolas Marchesotti, Daniele Magazzeni, and Manuela Veloso. Towards learning to explain with concept bottleneck models: mitigating information leakage. *ArXiv*, abs/2211.03656, 2022. URL <https://api.semanticscholar.org/CorpusID:253384003>.
- Warren M. Lord, Jie Sun, and Erik M. Bollt. Geometric k-nearest neighbor estimation of entropy and mutual information. *Chaos: An Interdisciplinary Journal of Nonlinear Science*, 28(3):033114, 03 2018. ISSN 1054-1500. doi: 10.1063/1.5011683. URL <https://doi.org/10.1063/1.5011683>.
- Scott M Lundberg and Su-In Lee. A unified approach to interpreting model predictions. In *Advances in neural information processing systems (NeurIPS)*, pages 4765–4774, 2017.
- Anita Mahinpei, Justin Clark, Isaac Lage, Finale Doshi-Velez, and Weiwei Pan. Promises and pitfalls of black-box concept learning models. *CoRR*, abs/2106.13314, 2021. URL <https://api.semanticscholar.org/CorpusID:235652059>.
- Mikael Makonnen, Moritz Vandenheert, Sonia Laguna, and Julia E Vogt. Measuring leakage in concept-based methods: An information theoretic approach, 2025. URL <https://arxiv.org/abs/2504.09459>.
- Andrei Margeloiu, Matthew Ashman, Umang Bhatt, Yanzhi Chen, Mateja Jamnik, and Adrian Weller. Do concept bottleneck models learn as intended?, 2021. URL <https://arxiv.org/abs/2105.04289>.

- Loic Matthey, Irina Higgins, Demis Hassabis, and Alexander Lerchner. dsprites: Disentanglement testing sprites dataset. <https://github.com/deepmind/dsprites-dataset/>, 2017.
- Angelos Ragkousis and Sonali Parbhoo. Tree-based leakage inspection and control in concept bottleneck models, 2024. URL <https://arxiv.org/abs/2410.06352>.
- Naveen Raman, Mateo Espinosa Zarlenga, Juyeon Heo, and Mateja Jamnik. Do concept bottleneck models obey locality? In *XAI in Action: Past, Present, and Future Applications*, 2023. URL <https://openreview.net/forum?id=F6RPYDUIZr>.
- Marco Tulio Ribeiro, Sameer Singh, and Carlos Guestrin. "why should i trust you?" explaining the predictions of any classifier. In *Proceedings of the 22nd ACM SIGKDD international conference on knowledge discovery and data mining (KDD)*, pages 1135–1144, 2016.
- Muhammad Ridzuan, Mai A. Shaaban, Numan Saeed, Ikboljon Sobirov, and Mohammad Yaqub. Hulp: Human-in-the-loop for prognosis. In Marius George Lingurar, Qi Dou, Aasa Feragen, Stamatia Giannarou, Ben Glocker, Karim Lekadir, and Julia A. Schnabel, editors, *Medical Image Computing and Computer Assisted Intervention – MICCAI 2024*, pages 328–338, Cham, 2024. Springer Nature Switzerland. ISBN 978-3-031-72086-4.
- Yoshihide Sawada and Keigo Nakamura. Concept bottleneck model with additional unsupervised concepts. *IEEE Access*, 10:41758–41765, 2022. URL <https://api.semanticscholar.org/CorpusID:246485723>.
- Ramprasaath R Selvaraju, Michael Cogswell, Abhishek Das, Ramakrishna Vedantam, Devi Parikh, and Dhruv Batra. Grad-cam: Visual explanations from deep networks via gradient-based localization. In *Proceedings of the IEEE international conference on computer vision (ICCV)*, pages 618–626, 2017.
- Ivaxi Sheth and Samira Ebrahimi Kahou. Auxiliary losses for learning generalizable concept-based models. In *Proceedings of the 37th International Conference on Neural Information Processing Systems, NIPS '23*, Red Hook, NY, USA, 2023. Curran Associates Inc.
- Divyansh Srivastava, Ge Yan, and Tsui-Wei Weng. VLG-CBM: Training concept bottleneck models with vision-language guidance. In *The Thirty-eighth Annual Conference on Neural Information Processing Systems*, 2024. URL <https://openreview.net/forum?id=Jm2aK3sDJD>.
- Moritz Vandenhirtz, Sonia Laguna, Ričards Marcinkevičs, and Julia E Vogt. Stochastic concept bottleneck models. In *The Thirty-eighth Annual Conference on Neural Information Processing Systems*, 2024. URL <https://openreview.net/forum?id=iSjqTQ5S1f>.
- Xinyue Xu, Yi Qin, Lu Mi, Hao Wang, and Xiaomeng Li. Energy-based concept bottleneck models: Unifying prediction, concept intervention, and probabilistic interpretations. In *The Twelfth International Conference on Learning Representations*, 2024. URL <https://openreview.net/forum?id=I1quoTXZzc>.

Chih-Kuan Yeh, Been Kim, Serkan Arik, Chun-Liang Li, Tomas Pfister, and Pradeep Ravikumar. On completeness-aware concept-based explanations in deep neural networks. In H. Larochelle, M. Ranzato, R. Hadsell, M.F. Balcan, and H. Lin, editors, *Advances in Neural Information Processing Systems*, volume 33, pages 20554–20565. Curran Associates, Inc., 2020. URL https://proceedings.neurips.cc/paper_files/paper/2020/file/ecb287ff763c169694f682af52c1f309-Paper.pdf.

Mert Yuksekgonul, Maggie Wang, and James Zou. Post-hoc concept bottleneck models. In *The Eleventh International Conference on Learning Representations*, 2023. URL <https://openreview.net/forum?id=nA5AZ8CEyow>.

Bolei Zhou, Aditya Khosla, Agata Lapedriza, Aude Oliva, and Antonio Torralba. Learning deep features for discriminative localization. In *Proceedings of the IEEE conference on computer vision and pattern recognition (CVPR)*, pages 2921–2929, 2016.